IMPROVING THE PERFORMANCE OF A COMMUNICATION VIA DIFFUSION SYSTEM CONSIDERING MOLECULE DEGRADATION IN NANONETWORKING

by

Fatma Nur Kılıçlı

B.S., Computer Engineering, Boğaziçi University, 2013

Submitted to the Institute for Graduate Studies in
Science and Engineering in partial fulfillment of
the requirements for the degree of
Master of Science

Graduate Program in Computer Engineering

Boğaziçi University

2015

ACKNOWLEDGEMENTS

I would like to express my sincere gratitude to all those who gave me the power to complete this thesis. All work done here is dedicated to the ones who reluctantly or confidently couldn't reach the end of this arduous path.

First of all, I would like to thank to my thesis supervisor Prof. Tuna Tuğcu for many enlightening suggestions and guidance during the development of this thesis. I am grateful to Prof. Fatih Alagöz and Assist. Prof. Bahri Atay Özgövde for their insightful and leading comments and also for their participation in my thesis committee.

I offer my deepest thanks to my colleagues Şükrü, Birkan, Salim, Ali, Gaye, Akif, Burcu, and Tuğrul for their ideas, collaboration, and help. Also, I would like to thank to current and former members of NETLAB and SATLAB for supports and confabulations during this period.

I am indebted to my close friends, especially Doğansel and İlke, for bearing me in my ups and downs. They were really uplifting and caring throughout this stage.

Last but not least, I would like to thank my family for their love, patience, and support in every sense. Without them, it would be literally impossible to finish this thesis.

This thesis is partially supported by the Scientific and Technical Research Council of Turkey (TUBITAK) under grant number 112E011, Bogazici University Research Fund (BAP7436), and the State Planning Organization (DPT) of the Republic of Turkey under the project TAM with the project number 2007K120610.

ABSTRACT

IMPROVING THE PERFORMANCE OF A COMMUNICATION VIA DIFFUSION SYSTEM CONSIDERING MOLECULE DEGRADATION IN NANONETWORKING

The interconnection between the nanoscale circuit components, which is referred to as nanonetworking, is a hot topic for nearly a decade. Among the various approaches studied in the literature, we apply communication via diffusion (CvD) method. Despite its practicality and ease of implementation, CvD brings along its own drawbacks especially to the reliability of the system. In order to overcome these drawbacks, we consider molecule degradation, which the literature on molecular communication mostly overlooks, in this thesis. We evaluate the performance of this proposed model by simulations and by using analytical expressions. In the simulations, we demonstrate the positive effects of molecule degradation on basic communication metrics in this scale. In addition, we use the analytical formulas in selecting the proper values of degradation utilized system parameters for mitigating intersymbol interference and correctly demodulating the signal. In this sense, the number of stray molecules remaining in the inter-cellular environment from the previous symbol is limited not to exceed the predefined threshold value while the number of received molecules is bounded to be greater than it. In the subsequent analysis, we examine the effects on the data rate and the energy consumption of the overall system. Results demonstrate that the increase in the data rate and the decrease in the energy expenditure can be achieved using appropriate half-life values.

ÖZET

NANO AĞLARDA MOLEKÜL BOZUNMASINI KULLANAN DİFÜZYON İLE HABERLEŞME SİSTEMLERİNİN PERFORMANSINI İYİLEŞTİRME

Nano ağlar olarak tanımlanan, nano ölçekteki cihazlar arasındaki bağlantı, son yılların önemli çalışma alanlarından biri olarak değerlendirilmektedir. Bu tezde, nano ağlardaki haberleşmeyi sağlayabilme amacıyla konu ile ilgilenen araştırmacılar tarafından faydalanılan birçok yaklaşım arasından difüzyon ile haberleşme (DiH) seçilmiştir. Bu tezde, DiH sistemlerinin beraberinde getirdiği haberleşme problemlerinin üstesinden gelmek adına, moleküler haberleşme çalışmalarında çoğunlukla göz önünde bulundurulmayan molekül bozunması olgusu hesaba katılmaktadır. Önerilen modelin performansı benzetimler ve çözümsel ifadeler yardımıyla değerlendirilmektedir. Benzetimlerde, molekül bozunmasının bazı temel nano boyuttaki haberleşme ölçevleri üzerindeki faydaları gösterilmektedir. Bunun yanı sıra, semboller arası girişimin azalması ve gönderilen sinyalin doğru deşifre edilmesi amacıyla diğer haberleşme değiştirgeleri için belirlenen özgül değerlere bakılarak, molekül bozunmasını dikkate alan sistemlerin değişkenleri için uygun değer seçimi yapılmaktadır. Bir önceki sembolden kalan artık molekül miktarının önceden belirlenmiş bir eşik değerinin altında kalması ve alıcı hücreye varan taşıyıcı molekül sayısının bu değerin üzerinde olması, bu belirlemelerde kısıt olarak verilmiştir. Daha sonraki çözümlemede, molekül bozunmasının sistemin veri hızı ve enerji tüketimi üzerindeki etkileri incelenmektedir. Sonuçlar, uygun taşıyıcı molekül yarı-ömür değerleri kullanıldığında, veri hızının arttığını ve enerji harcamasının azaldığını göstermektedir.

TABLE OF CONTENTS

LIST OF FIGURES

LIST OF TABLES

LIST OF SYMBOLS

C	Channel capacity
C_0	Initial concentration of the messenger molecules
$C_{MM}(t)$	Concentration of the messenger molecules at time t
C_V	Number of messenger molecules carried by one vesicle
d	Distance between the transmitter and the receiver
D	Diffusion coefficient
E_C	Energy spent on carrying the vesicle to the cell membrane
E_E	Energy spent on the emission of the messenger molecule wave into the environment
$E[N^{Rx}(...)]$	Expected number of received molecules
$E[N_C^{Rx}]$	Expected number of received molecules emitted in the current symbol duration
$E[N_P^{Rx}]$	Expected number of received molecules emitted in the previous symbol duration
$E[N_{P_t}^{Rx}(S_i)]$	Total expected number of interference molecules regarding i^{th} previous symbol combination
$E[N^{ISI}(...)]$	Expected number of stray molecules
E_S	Energy spent on the synthesis of a single messenger molecule
E_T	Total energy consumption for transmission of symbol 1
E_V	Energy spent on the production of a vesicle
$F_{hit}(...)$	Probability of hitting to the receiver
$F_{ISI}(...)$	Probability of interference
$I(X;Y)$	Mutual information
k_B	Boltzmann constant
l	Distance from the center of the receiver to the transmitter
$\mathcal{N}$	Gaussian Distribution
N	Number of transmitted messenger molecules for symbol 1
N_0	Number of messenger molecules emitted for symbol 0
N_1	Number of messenger molecules emitted for symbol 1

$N_r(t)$	Number of received messenger molecules until time t
P_{c_0}	Probability of correct detection of 0
P_{c_1}	Probability of correct detection of 1
P_{e_0}	Probability of false detection of 0 as 1
P_{e_1}	Probability of false detection of 1 as 0
r	Stoke's radius
r_{NeN}	Radius of the nanonetworking-enabled nodes
r_{MM}	Radius of the messenger molecules
$\overrightarrow{r}$	Location of a messenger molecule
S_P	Previous symbol
S_i	i^{th} previous symbol combination
$t_{1/2}$	Degradation half-life
t_s	Symbol duration
T	Absolute temperature
$\mathcal{U}$	Uniform Distribution
X	Intended symbol
Y	Received symbol
Δt	Step size of messenger molecules
Δx	Displacement of the messenger molecule in the x-axis
ΔX	One dimensional displacement of a diffusing molecule
Δy	Displacement of the messenger molecule in the y-axis
Δz	Displacement of the messenger molecule in the z-axis
η	Viscosity of the communication environment
γ	Number of emitted molecules for corresponding symbol
λ	Rate of degradation
μ	Mobility of the messenger molecule
ρ	Uniformly distributed random variable
τ	Detection threshold
ζ	Frictional coefficient of the messenger molecule

LIST OF ACRONYMS/ABBREVIATIONS

1D	One Dimensional
3D	Three Dimensional
ACh	Acetylcholine
AChE	Acetylcholinesterase
AM	Amplitude Modulation
BCSK	Binary Concentration Shift Keying
BPS	Bits Per Second
CDF	Cumulative Distribution Function
CNT	Carbon Nanotube
CSK	Concentration Shift Keying
CvD	Communication via Diffusion
EM	Electromagnetic
GNR	Graphene Nanoribbon
Hh	Hedgehog
IC	Integrated Circuit
i.i.d.	Independently Identically Distributed
ISI	Intersymbol Interference
MM	Messenger Molecule
MoSK	Molecule Shift Keying
NeN	Nanonetworking-enabled Node
NMJ	Neuromuscular Junction
NO	Nitric Oxide
PDF	Probability Distribution Function
pH	Decimal logarithm of the reciprocal of the hydrogen ion activity in a solution
ROC	Receiver Operating Characteristic

1. INTRODUCTION

As the well-known Moore's law [1] states, the number of transistors on an Integrated Circuit (IC) doubles nearly every two years. Half a century after the law was stated, increasing the number of transistors reached a limit that requires an enlargement in chip sizes [2]. There are several disadvantages of this enlargement such as the increase in the weight. Meeting this limit with the current IC technology brings about the need for a further downsizing in circuit components as a solution to the problem. Microscale components are scaling down to nanoscale in order to accomplish the future needs of the developing technologies [3]. These reasons give rise to a novel area of study: nanotechnology.

Nanotechnology is about systems in nanoscale, which refer to the systems that have at least one dimension of less than 100 nanometers ($10^{-7} meters$). It has numerous application areas such as biomedical engineering, environmental sciences, industry, multimedia, and military [4]. It has been a trending topic for a few decades. Being a new field, currently, the studies focus on very basic needs of the communication environment and the tasks of the nanomachines, which are built from the nanoscale components. As their sizes get smaller, the capability range of these nanomachines narrows down. Nanomachines are considered to be able to execute simple computing and sensing tasks [4].

In order to accomplish more complex tasks, nanomachines need to communicate with other nanomachines in the vicinity and also with higher scale machines. All of these necessities call forth another field of research concerning the interconnection among nanomachines, i.e. nanonetworking, where more complex tasks are handled via exchanging information between nanomachines [4]. In the literature, there are various approaches for nanonetworking such as the usage of acoustic, heat, molecule, or electromagnetic waves [5]. In this thesis, we focus on molecular communication inspired by the biological systems, where the communication is handled via the usage of messenger molecules (MMs) between biological transmission couples [6].

Among several methods in molecular communication, we employ communication via diffusion (CvD) since diffusion is a simple propagation method and there is no need for an external energy source or an additional infrastructure. In this approach, the transmitter and the receiver NeNs are located in the transmission medium where the information carrying MMs naturally disperse through. The transmitter NeN releases an MM wave into the environment according to the information to be sent. The reception of the MMs starts a series of chemical reactions on the receiver side, resulting in decoding of the information sent by the transmitter.

One of the most crucial drawbacks of CvD systems is the high intersymbol interference (ISI) caused by the random walk of the MMs. In order to mitigate ISI, several approaches have been taken in the literature [7, 8]. In most of the former studies, it is assumed that the messenger molecules always remain in the environment without any conformational change. However, when employed in the biological domain, every biodegradable molecule is degraded with a specific rate [9].

Degradation, enzymatically or non-enzymatically, is overly utilized in biological signaling systems. In the nanonetworking literature, the studies considering degradation in molecular communication are scarce, but it is very important in analyzing CvD environments and has to be incorporated into the molecular communications studies. Nakano et al. and Arifler et al. have analysed the channel capacity of a 1D CvD system considering non-enzymatic degradation [10,11]. They model the molecular degradation with exponential and Weibull distributions, respectively. On the other hand, Noel et al. consider enzymatic degradation in [12]. This model covers the enzyme-substrate confrontation problem in a 3D CvD system. However, the authors simplify the channel analysis by focusing on one symbol transmission and not considering ISI.

In this thesis, we apply this biological phenomenon into our CvD system in order to enhance the communication especially in terms of noise reduction. We examine the effect of exponentially distributed non-enzymatic molecule degradation in 3D CvD systems via simulations and using analytical formulas. We assume that the MMs does not travel among the communication environment forever, instead, they degrade by

themselves within this wandering duration. In the simulations, we use degradation to our advantage, to reduce the number of stray molecules in the communication. We evaluate the performance of the proposed scheme for different half-lives of different MMs and show that, by selecting the demodulation threshold cleverly, both ISI and the probability of false alarm decrease dramatically with higher rates of degradation [13].

In the analytical part, we limit the CvD system in order to be able to measure the effects of non-enzymatically degrading MMs. We have two boundary conditions for the number of the received MMs and the number of the stray MMs. We limit the received MMs to be greater than the threshold while the number of stray molecules to be less than it in order to have a reliable system. According to these bounds, we demonstrate how the values of the communication parameters are affected. Additionally, we focus on energy consumption and data rate of the overall system using analytical formulas. The results show that the proper utilization of degradation yields improvements in these metrics.

1.1. Contribution of this thesis

Main contributions of this thesis can be outlined as:

(i) *Effects of non-enzymatic degradation on communication*: We have simulated the CvD system with non-enzymatically degrading MMs and show its positive effects on various communication metrics against CvD systems that do not consider degradation.

(ii) *Parameter tuning in CvD with MM degradation for ISI cancelling*: We have demonstrated the selection of the values of different parameters for ISI mitigation and detection probability improvement. We have focused on the effects of degradation utilizing system parameters on communication metrics using analytical expressions.

(iii) *Increasing the data rate and diminishing the energy consumption in CvD with MM degradation*: We have shown the positive and the negative impact of degradation on data rate and the energy expenditure of CvD systems with variable

parameter value combinations.

1.2. Outline of this thesis

In this thesis, we focus on improving the performance in terms of selecting the optimal values of communication parameters in Communication via Diffusion (CvD) systems considering molecule degradation. Initially, in Chapter 3, we outline the details of the system model via describing the motion of the messenger molecules (MMs), modulation technique, channel characteristics, the energy cost, and the analytical model of CvD system with degrading MMs. In Chapter 4, we simulate the described scenario and show the effects of degradation on some communication performance metrics. In Chapters 6 and 7, we cope with the selection of parameter values in the sense of intersymbol interference mitigation, data rate maximization, and the minimization of the energy spent on the production of the messenger molecules. Finally, Chapter 8 concludes this thesis while providing some future works based on this topic.

2. BACKGROUND INFORMATION

2.1. Nanonetworking

Nanotechnology is a field of study concerning nanoscale systems. Nanomachines are nanoscale machines with the capability of executing simple tasks such as computing and sensing. An individual nanomachine can perform limited operations and needs to communicate with other nanomachines in the vicinity. As a novel area of study, nanotechnology gives rise to many research branches. One of them is nanonetworking, i.e. the interconnection of nanonetworking-enabled nodes (NeNs), which is a communication network that helps information exchange among nanoscale machines to achieve complex tasks [14].

In the literature, there are various approaches for nanonetworking such as the usage of acoustic, heat, molecule, or electromagnetic (EM) waves [5, 15]. In acoustic communication, the information is embedded in sound waves. The use of these waves in information transmission in nanoscale is an appropriate approach for underwater communication since these waves propagate over long distances within aqueous environment [16]. Heat wave transmission between the communication pairs utilizes the heat change in order to exchange information [16]. Molecular communication, which is similar to heat communication, encodes the information on a wave of molecules [4]. EM wave communication in nano scale, i.e. nano-electromagnetic communication, is analogous to the classical wireless communication, and based on the transmission and reception of EM radiation [17].

Among these approaches the nanonetworking literature currently focuses on nano-EM communication and molecular communication. In nano-EM, the transmission of EM waves in different frequencies requires too much energy while the reception is relatively easier. Thus, nano-EM communication is a promising method for information transmission from higher scales to nano scale [5]. Current research topics in this type of communication are comprised of developing channel models and protocol suites

for Terahertz band, examining Carbon Nanotubes (CNT) and Graphene Nanoribbons (GNR), and information modulation techniques [15, 17–19]. In molecular communication, which is inspired from the biological systems, the communication is handled via the usage of messenger molecules (MMs) as messengers between biological transmission couples [5]. Among these approaches, we focus on molecular communication in this thesis.

2.2. Molecular Communication

In the biology literature, various cellular communication methods for different communication ranges have been observed [20]. For instance, micro-tubule communication (molecular motors) is an example of short range communication; flagellated bacteria, ion signaling and communication via diffusion are examples of short to medium range communication; pheromone, spore, and pollen-based communications are examples of long range communications [20,21]. Among these various molecular communication methods, we choose to focus on the most basic one, Communication via Diffusion (CvD), due to its simplicity in modelling and low energy requirements.

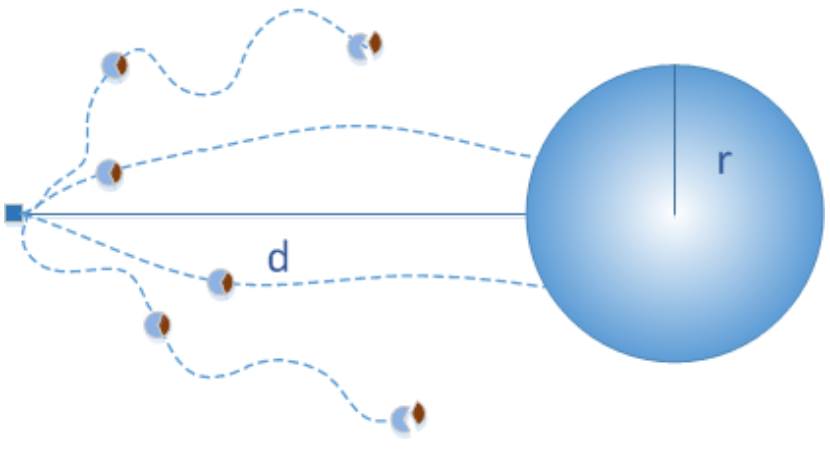

Figure 2.1. CvD system with a point source transmitter NeN and a sphere receiver NeN (Courtesy of [13]).

Utilizing the diffusion, cell-to-cell communication is handled by signaling systems

in the biology domain. These systems, which are classified as juxtacrine signals, endocrine signals, and paracrine signals [22], differ according to their physical properties such as activity ranges and messenger types.

The main difference between these signaling systems is their communication ranges. In juxtacrine signaling, the transmitter and the receiver are adjacent and MMs are transfered from their contact point [23]. Hence, it does not let the communication pair to be distant, which is not practical for most systems. In endocrine signaling, in contrast, the distance between the transmitter and the receiver is large. MMs of endocrine signaling, i.e. hormones, travel a long distance to reach to the receiver, which causes the communication to be slow and the effect on the receiver side to be lasting [9]. The third choice, paracrine signaling, requires a shorter distance than endocrine signaling and less time for the effect on the receiver side to vanish [9]. Those properties make paracrine signaling a better choice to be imitated in the studies.

2.2.1. Communication via Diffusion (CvD)

In CvD, the main communication components are the transmitter NeN, the receiver NeN, and MMs. Here, the transmitter and the receiver cells, which are called as Nanonetworking-enabled Nodes (NeNs), are located in the transmission medium where the information carrying MMs propagate through. We model a system that is composed of a 3D fluid communication environment, a point source as the transmitter, and a spherical NeN device as the receiver (Figure 2.1). The transmitter NeN releases an MM wave into the environment according to the information to be sent, namely the *intended symbol* [24]. Emitted MMs' motion within the communication environment is ruled by diffusion dynamics until being received by the receiver NeN. MMs are received with the help of the receptors placed on the surface of the receiver body. This reception within a given amount of time, i.e. symbol duration (t_s), starts a series of chemical reactions at the receiver side and results in decoding the information sent by the transmitter NeN [6]. This decoding results in the so-called *received symbol*. A successful communication is achieved only when the intended symbol is the same as the received symbol.

In CvD, there are five main steps of communication: modulation, transmission, propagation, reception, and demodulation.

- *Modulation*: In this step, the transmitter NeN modulates the information in the MM wave using a specific technique, which is also known by the receiver.
- *Transmission*: This step includes the emission of the MM wave by the transmitter from its membrane to the environment. Since we have a point source in this model, all MMs start travelling from the same point.
- *Propagation*: After the MM wave is emitted to the environment, all molecules constituting the wave start to diffuse according to Brownian motion.
- *Reception*: Some of the MMs are captured by the receptors of the receiver NeN in this step. Note that Brownian motion does not guarantee that all MMs will reach at the receiver.
- *Demodulation*: In this step, the receiver NeN estimates the information sent by transmitter using a predefined technique that is identical to the one used by the transmitter NeN in the modulation phase.

Due to the dynamics of the medium, the transmitter should send a high number of MMs to achieve a reliable transmission. This leads to a lot of MMs being wasted, which in turn increases the energy cost of the communication system. Since the reception of MMs by the receiver spreads over a long period of time, there are MMs wandering within the environment after t_s [24]. These MMs reach at the receiver in subsequent t_s's and may cause erroneous decoding of the information [25]. Additionally, the propagation speed of the signal in the CvD medium is comparably slower than the signal speed of traditional wired and wireless communication systems. Another important issue in this medium is the inability to differentiate between the arrival of MMs emitted at different times [12]. This issue causes Intersymbol Interference (ISI) in the CvD system.

There are several works based on ISI mitigation [7,8,26–28]. For the CvD system, the general aspect of the former studies where ISI was considered is based on the

assumption that MMs always remain within the communication environment without any conformational change. However, in the biology domain, it is observed that every biodegradable molecule is degraded with a specific rate [9]. In order to mitigate ISI, the molecular degradation can also be utilized [13,29]. In [13], the effect of degradation on ISI is shown for various degradation rates. This study concludes that ISI decreases with increasing rate of degradation.

2.3. Molecule Degradation

In biological systems, metabolites, drugs, messenger molecules, and many other substances have the property of degradation. The usage of biodegradable materials in various medical applications goes back to the beginning of 1960s [30]. Any drug utilized in medical treatments has a specific rate of degradation, i.e. λ, which also determines the treatment schedule of the patient [31].

The time required for the concentration of a molecule within the environment to drop by half is defined as the *half-life* [9]. Half-life times, denoted by $t_{1/2}$, are widely spread from milliseconds to years for different types of molecules [32]. For example, hexadecadienyl acetate pheromone has an estimated half-life of 15 milliseconds, and the half-life of nitric oxide (NO), which is an important signaling molecule in mammals, is 2-6 seconds whilst this parameter is 5.5 months for bedaquiline and 30 years for Cadmium in bones [9,32].

In the cellular scale, molecule degradation has many benefits for both the cell and the environment. These advantages can be listed as the elimination of the damaged molecules, recycling of building blocks of the molecule, prevention of a irregular concentration increase, protection against the formation of undesired molecules, etc. [9,33] Particularly for the molecules utilized in quick response to external stimuli, degradation and turnover rates allow the cell to adapt the changes [22].

Molecules are inactivated by a structural deformation caused by reactions such as phosphorylation, cleavage, ubiquitination, acetylation, formylation, and glycosylation

[34]. For proteins, the breakdown process is called as *proteolysis* and achieved both intracellularly and extracellularly. This process, in the biology domain, can be achieved by enzymatic and non-enzymatic methods as detailed in the following sections [33].

2.3.1. Enzymatic Degradation

In enzymatic degradation, a specific enzyme changes the structure of the substrate, which is MM in our CvD system. Enzymes have an *active site* that causes a conformational change in the substrate (see Figure 2.2). The enzymes, also, have biological half-lives, but compared to their substrates, half-lives of the enzymes are shorter. These biological materials can perform their activities for many times; that is, there is no upper limit in the number of molecules that is degraded by one enzyme [35].

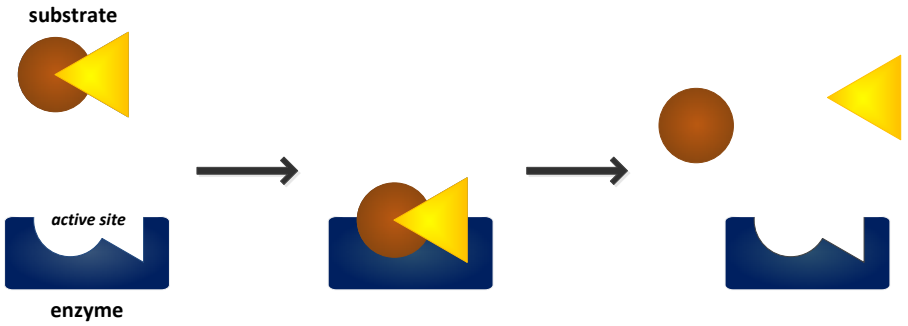

Figure 2.2. Degradation of a molecule by a specific enzyme. Enzyme's inner surface (i.e. active site) causes a conformational change in the substrate.

In this type of degradation, enzyme concentration controls the degradation rate. The more the number of enzymes within the environment, the faster the substrates degrade. Enzyme usage affects the half-life values, and thus, the substrate concentration changes. Such controlling of the substrate concentration with the help of enzymes is seen as a *negative feedback loop* procedure in biology. In most of the biological signaling examples, there is a self-control system. The release of the signal stimulates the production of a primary molecule. The increase of this molecule within the communication environment triggers the production of a secondary molecule, which affects the signal in reverse direction (Figure 2.3).

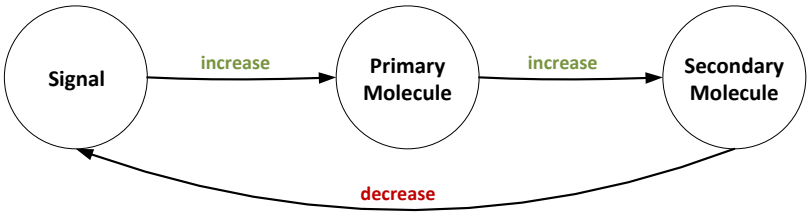

Figure 2.3. Negative feedback loop.

The signal itself produces the primary molecule in order to transmit the information or trigger a stimuli. The emitted molecules wander within the environment and are caught by the receiver. The received molecules provoke the receiver to increase another molecule's concentration (secondary molecule). These produced molecules inhibit the signal, thus, decrease primary molecule production. This kind of secondary molecule utilizations are widely observed in cell signaling. Looking at these systems from a molecular communications point of view, the increase in the primary molecules corresponds to the increase in the residual molecules from the previous symbols. The noise, i.e. ISI in CvD, caused by these molecules is smothered by the secondary molecules in order to control the information flow.

In the biochemistry literature, many models exist for enzymatic reactions. Among these models, the Michaelis-Menten kinetics indicates that the enzymatic reactions depends on the substrate concentration [36]. Basically, when the concentration of the degrading enzyme increases, the degradation rate also increases (Figure 2.4). This increase in the rate causes a decrease in the substrate concentration that decreases the degradation rate. As a result, the degradation of the substrate is time-variant in the existence of enzymatic reactions.

One of the good examples of enzymatic degradation is the communication between the neuron and the muscle cell in the neuromuscular junction (NMJ) [37]. In NMJ, Acetylcholine (ACh) is used as the MM of the communication, and its concentration is controlled by the enzyme called Acetylcholinesterase (AChE). Non-enzymatic

elimination half-life ($t_{1/2}$) of ACh is 2 minutes [38]. With the usage of AChE, which is one of the fastest enzymes, $t_{1/2}$ of ACh is diminished down to 1-2 milliseconds [39].

In the biology domain, the enzyme does not always degrade the substrate when they come across. The degradation reaction requires an activation energy. Thus, if there is a lack of energy, the enzyme releases the substrate without causing any conformational change to it. Adding the probability of meeting the enzyme in 3D, in the first place, communication becomes more complicated.

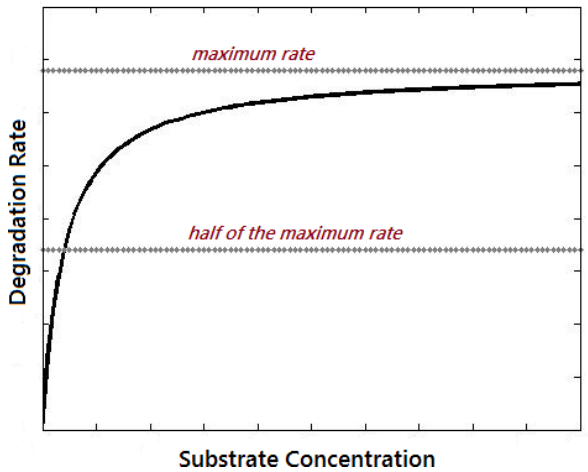

Figure 2.4. Michaelis-Menten kinetics enzymatic reaction rate vs. substrate concentration curve.

2.3.2. Non-enzymatic Degradation

In the nature, in vitro studies indicate the presence of auto-degrading biological materials in the absence of corresponding enzymes. In this kind of degradations, called the non-enzymatic degradations, molecules are degraded without the help of any external molecules, which can be referred as a self-elimination. These degradations can emerge from changes in the temperature, pH, and many other chemical substances in the environment.

Non-enzymatic degradation can be counted as a simpler form of enzymatic degra-

dation since there is only the half-life value to control the molecule concentration as opposed to the dynamics existing in enzymatic degradation, such as Michaelis-Menten kinetics and enzyme affinity. In this type of degradation, the number of molecules in the environment can be represented by a generic time-varying exponential decay function,

$$C_{molecule}(t) \;=\; C_0 e^{-t\lambda} \tag{2.1}$$

where C_0 is the initial concentration of the corresponding substrate, $C_{molecule}(t)$ is the concentration at time t, and λ is the degradation rate. In exponential decay, the time required for the initial concentration to drop by half is defined as half-life. This is exactly the same definition of half-life as in molecule degradation. Thus, in this non-enzymatic degradation model, $t_{1/2}$ value is calculated as:

$$t_{1/2} \;=\; \frac{ln(2)}{\lambda}. \tag{2.2}$$

Additionally, cumulative distribution function (cdf) of the exponential represents the total number of molecules degraded until a given amount of time. So the inverse cdf, i.e. the quantile function, given in Equation 2.3, can be used in defining the time required for the degradation of a fraction of molecules (ρ) for a given degradation rate value,

$$\mathcal{F}^{-1}(\rho;\lambda) \;=\; -\frac{ln(1-\rho)}{\lambda} \tag{2.3}$$

where $0 \leq \rho < 1$.

2.3.3. Degradation in Molecular Communication

In the literature, molecule degradation in the molecular communication has not been studied extensively. Nakano *et al.* [10] and Arifler *et al.* [11] have analysed the

channel capacity of a one dimensional receiver CvD system considering non-enzymatic degradation. They model the molecular degradation with exponential and Weibull distributions respectively. On the other hand, Noel *et al.* consider enzymatic degradation in [12,29]. This model covers the enzyme-substrate confrontation problem in a 3D CvD system. However, the authors simplify the channel analysis by focusing only on one symbol transmission and not considering ISI. In addition, Heren *et al.* represent the analytical modelling of the CvD system with a 3D receiver considering MM degradation in [40]. They derive the formulas for detection and reception probabilities while showing the effects on important metrics of the communication. We give more details of this paper in the following sections and utilize the expressions clarified there.

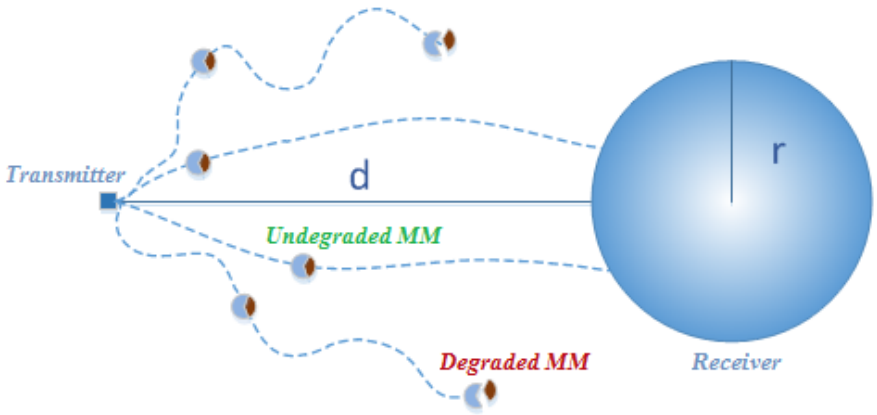

Figure 2.5. CvD system with degrading MMs in a point source transmitter NeN and a sphere receiver NeN communication environment.

Degradation, enzymatically or non-enzymatically, is overly utilized in biological signaling systems. Studies incorporating degradation in molecular communication, such as aforementioned works, increase. In this thesis, we also utilize degradation in 3D CvD systems. When degradation is applied to our CvD systems, after the conformational change, the receiver NeN cannot be able to recognize and capture the degraded MM as a part of the information sent. The receptors placed on the receiver body are designed to receive the undegraded MMs but not the degraded ones (Figure 2.5).

As detailed in the previous sections, in enzymatic degradation, the probability of MMs encountering the enzyme in the 3D environment should be considered. According to the type of the chemical reaction, the encountering angle and the velocity values of the substrate and the enzyme are important. Additionally, in order to be able to start the reaction, external energy is needed. To eliminate these complexities, we apply non-enzymatic degradation to our CvD system.

3. SYSTEM MODEL

As stated in the previous chapter, information exchange between NeNs is based on CvD in this thesis. In this communication method, MMs carry the information among the communicating pair via dispersing within the liquid environment. The motion of the MMs starting from the transmitter NeN targeting the receiver NeN is ruled by the dominant dynamics of this scale, i.e. diffusion. Adding degradation to the system, an MM can be degraded while wandering within the communication environment, however a degraded MM stops its motion within the environment. In this chapter, we provide a brief description of the propagation of the MMs and give details of our channel model.

3.1. Model for Propagation of the Messenger Molecules

Diffusion is a simple propagation method that does not require an external energy source, MMs move by themselves. Also, no additional infrastructure is required in diffusion, such as the microtubules used as railways in intracellular transportation by molecular motors. Free MMs naturally disperse through the communication environment over time.

In our communication environment, MMs are considered to move according to Brownian motion. Brownian motion, named after botanist Robert Brown, is defined as the stochastic movements of small particles suspended in a solution [41]. [1] The properties of this motion and diffusion dynamics are used in the formulation of the motion of MMs. The amount of time it takes for an MM to reach the receiver NeN varies for every MM and is affected mainly by the distance d between the transmission point and the receiver, and the diffusion coefficient D. Upon contact with the receiver NeN, an MM is received and removed from the communication environment.

In [21], it is stated that the collisions with other MMs have less effect to the subject MM compared to the forces applied by the molecules of the liquid if the number

[1] More detail about Brownian motion is available in Appendix A.

of MMs is apparently lower than the number of the liquid molecules. We assume that the MMs are much rare than the liquid molecules, thus, we omit the collisions between MMs while wandering within the environment.

In a 1D environment, the movement of a single MM in unit time Δt is a normally distributed random variable ΔX with zero mean and σ standard deviation

$$\Delta X \sim \mathcal{N}(\Delta X; 0, \sigma^2) \tag{3.1}$$

where $\sigma = \sqrt{2D\Delta t}$. The MMs in our model propagate through a 3D environment, where the movements in all dimensions are i.i.d. Gaussian variables [42]. Therefore the total displacement in single time step becomes

$$\overrightarrow{r} = (\Delta x, \Delta y, \Delta z). \tag{3.2}$$

3.2. Channel Model

In order to analyze the performance of the communication channel with degrading MMs, we set some baseline operation concepts. In Section 3.2.1, the modulation technique used in the simulations is examined. In this channel model, full-synchronization of the transmitter-receiver pair is assumed [43]. In Section 3.2.2, the channel capacity is calculated using the mutual information and the detection probabilities. Next, we explain the energy model for the calculation of energy expenditure of the overall system.

3.2.1. Modulation Technique

As explained before, the information exchange in CvD systems is handled via sending a sequence of symbols spread over time. We assume that the time is divided into time slots of equal size, i.e. the symbol duration, in which one symbol is sent. Numerous techniques can be used for utilizing this symbol duration for information

transmission, where the information is modulated over one or more physical properties of the MMs (e.g., concentration, frequency, molecule type) [10, 21, 44]. If the information is modulated onto the concentration of MMs, it is called Concentration Shift Keying (CSK) [24]. This is very similar to the Amplitude Modulation (AM) in classical communication systems and also Hedgehog (Hh) signaling that helps the evolution of the embryonic cells. The information can also be modulated onto the type of the molecule, which is called Molecule Shift Keying (MoSK) [44].

In the proposed model, we employ Binary Concentration Shift Keying (BCSK) as the signal modulation technique, where 1-bit symbol is sent in a symbol duration [44]. To transmit a symbol with a bit value of "1" or "0", the transmitter NeN erupts N_1 or N_0 number of molecules, respectively. In this thesis, we assume N_0 is zero and N_1 is N.

The receiver NeN counts the number of molecules arriving in a symbol duration. We denote this amount by $N_r(t)$, which shows the received number of molecules by time t. The receiver NeN compares this number with the predetermined threshold, τ. If $N_r(t_s)$ falls short of τ, the demodulated symbol value is considered to be "0", whereas if $N_r(t_s)$ exceeds τ, the demodulated symbol is accepted as "1".

3.2.2. Channel Capacity and Data Rate

The capacity of extracting information in the system via a thresholding mechanism depends on various parameters. Considering the CSK modulation and given the values of the parameters d, N_0, N_1, r_{NeN}, and D, the optimal value for τ can be defined as the value that maximizes the mutual information, which is defined as

$$I(X;Y) \;=\; \sum_{y\in Y}\sum_{x\in X} p(x,y)\log_2\left(\frac{p(x,y)}{p(x)p(y)}\right) \tag{3.3}$$

for a binary asymmetric channel. Here, $XandY \in \{0,1\}$ represent the intended symbol and the received symbol, respectively. In this equation log base-2 is used, in order to

get the mutual information in bits. The probability of a bit value of "0" and "1" are equally selected as $p(x=0) = p(x=1) = 0.5$. The reception probabilities are

$$p(y=1) \;=\; p(x=1)\cdot P_{c_1} + p(x=0)\cdot P_{e_0} \tag{3.4}$$

and

$$p(y=0) \;=\; p(x=0)\cdot P_{c_0} + p(x=1)\cdot P_{e_1} \tag{3.5}$$

where P_{c_1} and P_{c_0} are the correct detection probabilities, while P_{e_1} and P_{e_0} are the erroneous detection probabilities of corresponding symbols. Notice that for each bit $P_{c_0} + P_{e_0} = 1$ and $P_{c_1} + P_{e_1} = 1$ must hold. When these equalities are applied[2] , we calculate the mutual information in our model as

$$\begin{aligned} I(X;Y) \;=\; \frac{1}{2}\Bigg\{ & P_{c_0}\log_2\left(\frac{2P_{c_0}}{P_{c_0}+P_{e_1}}\right) + P_{e_0}\log_2\left(\frac{2P_{e_0}}{P_{e_0}+P_{c_1}}\right) + \\ & P_{c_1}\log_2\left(\frac{2P_{c_1}}{P_{c_1}+P_{e_0}}\right) + P_{e_1}\log_2\left(\frac{2P_{e_1}}{P_{e_1}+P_{c_0}}\right)\Bigg\} \end{aligned} \tag{3.6}$$

or

$$\begin{aligned} I(X;Y) \;=\; \frac{1}{2}\big[& 2 + P_{c_0}\log_2(P_{c_0}) + P_{e_0}\log_2(P_{e_0}) + P_{c_1}\log_2(P_{c_1}) + P_{e_1}\log_2(P_{e_1}) \\ & - (P_{c_0}+P_{e_1})\log_2(P_{c_0}+P_{e_1}) - (P_{e_0}+P_{c_1})\log_2(P_{e_0}+P_{c_1})\big]. \end{aligned} \tag{3.7}$$

Figure 3.1 demonstrates that the mutual information increases when P_{c_1} and P_{c_0} increase. In other words, P_{e_1} and P_{e_1} are expected to have small values in order to be able to have high mutual information. However, mutual information also increases with tiny P_{c_1} and P_{c_0} values. This attribute can be read as "having the wrong information leads the receiver to decide as the opposite of the received information". However, we focus on the other part of the graph where P_{c_1} and P_{c_0} have values higher than 0.9.

[2]See Appendix B for the derivation.

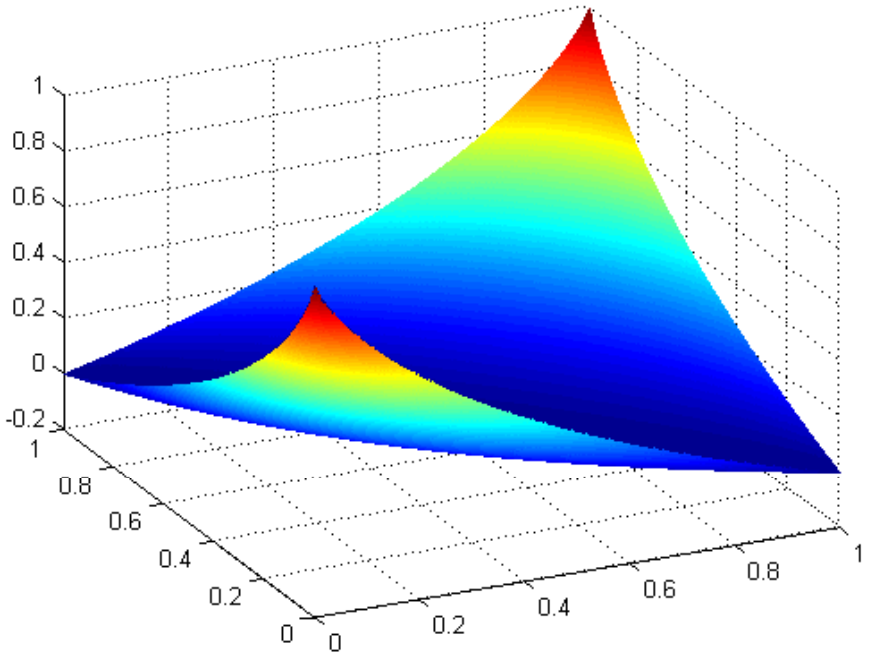

Figure 3.1. Mutual information change with P_{c_0} and P_{c_1}.

Channel capacity of the overall system, i.e. C, is the maximum value of the mutual information as in Equation 3.8. In order to maximize the mutual information, the proper value of τ should be chosen as the threshold of the model. The mutual information is a concave function and therefore has a global maxima, when plotted with respect to threshold values.

$$C = \max_{\tau} I(X;Y). \tag{3.8}$$

When the data rate is considered, the symbol duration should also be incorporated in the formula. The capacity of the system shows the information rate in bits. However, data rate (in BPS) considers how fast this information is transferred from the transmitter to the receiver. Thus, data rate is calculated as

$$data\,rate = \frac{C}{t_s} = \frac{\max_{\tau} I(X;Y)}{t_s}. \tag{3.9}$$

3.2.3. Energy Model

In order to achieve the communication, the transmitter NeN emits MMs into the environment in CvD model. Some of the previous works assume that these molecules are produced from their building blocks in the transmitter side. For example in [20], they calculate the total energy spent on one molecule wave similar to *exocytosis* in cell biology. They consider that the transmitter NeN produces MMs and release them from its membrane within vesicles carried by the molecular motors [9].

Thus, the transmitter spends energy on synthesis of a single MM (E_S), production of a vesicle (E_V), carrying the vesicle (E_C), and emitting the MM wave from the membrane (E_E). Thus, the total energy consumption of N molecules becomes:

$$E_T = N \cdot E_S + \left\lceil \frac{N}{C_V} \right\rceil (E_V + E_C + E_E) \tag{3.10}$$

where N is the number of emitted MMs for symbol value "1" and C_V is the number of MMs carried by one vesicle. When the size of the MM diminishes and other variables are fixed, the energy spent also decreases. However, for a specific communication setup, E_S, E_V, E_C, E_E, and C_V have specific values. Thus, the energy consumption of the system is directly proportional to N

$$E_T \propto N. \tag{3.11}$$

In Chapter 6, we focus on the energy expenditure of the systems considering MM degradation in 3D CvD. In this sense, we accept the total number of emitted molecules as the comparison metric between the systems with different degradation rates.

3.3. Analytical Model

In this section, we introduce the reception and interference probabilities of the CvD model considering molecule degradation analytically. Using these formulas we

define the probability of correct and erroneous demodulation of the signal. We use these analytical expressions in Chapter 5 for the calculations of the received and the stray molecules, and in Chapter 6 in order to demonstrate the effects of non-enzymatic degradation on data rate.

3.3.1. Probability of Reception

Across the distance d, MMs propagate through the communication environment. Since their motion is ruled by the diffusion dynamics, there is the probability of not arriving at the receiver within the intended time interval, i.e. the symbol duration. In [45], the probability of hitting to the receiver within t duration is shown as

$$F_{hit}(t \mid r_{NeN}, d, D) \;=\; \frac{r_{NeN}}{l}\, erfc\left(\frac{d}{\sqrt{4Dt}}\right), \tag{3.12}$$

where $l \;=\; d + r_{NeN}$ is the distance from the point source to the center of the spherical receiver body, and r_{NeN} is the radius of the receiver as mentioned in the previous sections. *erfc* function used in the above equation is the complementary error function, which is defined as

$$erfc(x) \;=\; \frac{2}{\sqrt{\pi}} \int_{x}^{\infty} e^{-t^2} dt. \tag{3.13}$$

Each MM is subject to an independent Bernoulli trial. Since their probabilities of being received are equal, the process is Bernoulli sampling. Since each MM is considered separately, the total number of received molecules follows a Binomial distribution, which is the distribution of the sum of Binomial trials each with the same probability. Therefore, using Equation 3.12, the expected number of molecules received by the receiver until time t can be calculated as multiplying the probability with the number of emitted molecules,

$$E\left[N^{Rx}(t \mid r_{NeN}, d, D, N)\right] \;=\; \gamma \;\cdot F_{hit}(t \mid r_{NeN}, d, D) \tag{3.14}$$

where γ is the number of emitted MMs from the transmitter, which depends on the symbol value. In other words, when the symbol is "0", the number of emitted MMs is zero, i.e. $\gamma = 0$, according to the modulation technique used here. Conversely, if the symbol is "1", $\gamma = N$.

$$\gamma = \begin{cases} N & \text{if } \textit{the symbol is } 1 \\ 0 & \text{if } \textit{the symbol is } 0. \end{cases} \tag{3.15}$$

However, Equation 3.12 and 3.14 ignore MM degradation. When degradation is considered in the CvD system, these hitting probabilities change due to the decrease in the number of MMs on their way to the receiver. Some MMs are degraded within the symbol duration causing a decrease in the probability of receiving by the receiver NeN. In [40], this new probability of reception is calculated as

$$\begin{aligned} F_{hit}(t, \lambda \mid r_{NeN}, d, D) \; = & \frac{r_{NeN}}{2l} \exp\left(-d\sqrt{\frac{\lambda}{D}}\right) \left\{1 - erf\left(\frac{d}{\sqrt{4Dt}} - \sqrt{\lambda t}\right)\right. \\ & \left. + \exp\left(2d\sqrt{\frac{\lambda}{D}}\right)\left[1 - erf\left(\frac{d}{\sqrt{4Dt}} + \sqrt{\lambda t}\right)\right]\right\}. \end{aligned} \tag{3.16}$$

When $t \to 0$, the probability of being received by the receiver is zero as expected. On the other limiting condition, $t \to \infty$, the probability is less than one and inversely proportional to the degradation rate since some of the MMs are degraded over time. As in Equation 3.14, multiplying this probability with the number of transmitted molecules gives the expected number of received molecules within t

$$\begin{aligned} E\left[N^{Rx}(t, \lambda \mid r_{NeN}, d, D, N)\right] \; = & \gamma \frac{r_{NeN}}{2l} \exp\left(-d\sqrt{\frac{\lambda}{D}}\right) \left\{1 - erf\left(\frac{d}{\sqrt{4Dt}} - \sqrt{\lambda t}\right)\right. \\ & \left. + \exp\left(2d\sqrt{\frac{\lambda}{D}}\right)\left[1 - erf\left(\frac{d}{\sqrt{4Dt}} + \sqrt{\lambda t}\right)\right]\right\} \end{aligned} \tag{3.17}$$

where λ is the degradation rate and $erf(x)$ is the error function. Providing that $erf(x)+$

$erfc(x) = 1$, the error function equals to

$$erf(x) \;=\; \frac{2}{\sqrt{\pi}} \int_0^x e^{-t^2} dt, \tag{3.18}$$

which converges to 1 when $x \to \infty$ and to -1 when $x \to -\infty$.

3.3.2. Probability of Interference

Applying degradation into our communication environment also causes a decrease in the number of stray molecules as shown in the simulation results in Section 4.2. Using the analytical formulas in the previous section, it is possible to calculate the fraction of the non-received molecules within t. When the fraction of the received molecules is calculated for $t \to \infty$, it gives the total probability of being received by the receiver. The difference between $F_{hit}(t \to \infty, \lambda \mid r_{NeN}, d, D)$ and $F_{hit}(t, \lambda \mid r_{NeN}, d, D)$ gives the probability of being received after t. Dividing it to the total probability, $F_{hit}(t \to \infty, \lambda \mid r_{NeN}, d, D)$, results in the fraction of stray molecules that refer to the molecules causing ISI in the following symbol durations [40]:

$$\begin{aligned} F_{ISI}(t, \lambda \mid d, D) \; &= 1 - \frac{F_{hit}(t, \lambda \mid d, D)}{F_{hit}(t \to \infty, \lambda \mid d, D)} \\ &= \frac{1}{2} \left\{ 1 + erf\left(\frac{d}{\sqrt{4Dt}} - \sqrt{\lambda t} \right) - \exp\left(2d\sqrt{\frac{\lambda}{D}} \right) \right. \\ &\quad \left. \times \left[1 - erf\left(\frac{d}{\sqrt{4Dt}} + \sqrt{\lambda t} \right) \right] \right\}. \end{aligned} \tag{3.19}$$

Similar to Equation 3.17, the expected number of MMs within the environment without being degraded after t amount of time of being released is

$$\begin{aligned} E\left[N^{ISI}(t, \lambda \mid d, D, N) \right] \; &= \gamma \, \frac{1}{2} \left\{ 1 + erf\left(\frac{d}{\sqrt{4Dt}} - \sqrt{\lambda t} \right) - \exp\left(2d\sqrt{\frac{\lambda}{D}} \right) \right. \\ &\quad \left. \times \left[1 - erf\left(\frac{d}{\sqrt{4Dt}} + \sqrt{\lambda t} \right) \right] \right\}, \end{aligned} \tag{3.20}$$

where $N^{ISI}(t, \lambda \mid d, D)$ shows the number of stray molecules within the environment without being degraded or captured by the receiver after t. These interference molecules are expected to be received by the receiver after t, that is, they compose the residual molecules causing ISI by arriving at the receiver within the following symbol durations.

3.3.3. Probability of Detection

As mentioned earlier, due to their random motion, some of the MMs arrive at the receiver not within the intended symbol duration, but in the following symbol durations. This may cause the erroneous demodulation of the signal. When degradation is considered, the number of received molecules decreases and the probability of correctly detecting the transmitted symbol changes.

The number of received molecules within one symbol duration depends not only on the current symbol, but also on the previous transmitted symbols. For instance, when we consider the stray molecules remaining from only one previous symbol duration, we calculate the detection probabilities as follows:

$$\begin{aligned}
P_{c_1} &= p(S_P = 0)\, p(E[N_C^{Rx}] \geq \tau) + p(S_P = 1)\, p(E[N_P^{Rx} + N_C^{Rx}] \geq \tau) \\
P_{c_0} &= p(S_P = 0)\, p(0 < \tau) + p(S_P = 1)\, p(E[N_P^{Rx}] < \tau) \\
P_{e_1} &= p(S_P = 0)\, p(E[N_C^{Rx}] < \tau) + p(S_P = 1)\, p(E[N_P^{Rx} + N_C^{Rx}] < \tau) \\
P_{e_0} &= p(S_P = 0)\, p(0 \geq \tau) + p(S_P = 1)\, p(E[N_P^{Rx}] \geq \tau)
\end{aligned} \tag{3.21}$$

where P_{c_1} and P_{c_0} are the correct detection probabilities, while P_{e_1} and P_{e_0} are the erroneous detection probabilities of the corresponding symbols. Notice that for each bit, $P_{c_0} + P_{e_0} = 1$ and $P_{c_1} + P_{e_1} = 1$ must hold. Also, S_P denotes the value of the previous symbol in the equations above. Also, the expected number of MMs from previous symbol duration, i.e. $E[N_P^{Rx}]$, is $N \cdot [F_{hit}(2t_s, \lambda \mid r, d, D) - F_{hit}(t_s, \lambda \mid r, d, D)]$, if the previous symbol is "1". Otherwise, since no molecules are emitted for symbol "0", we do not expect to receive any molecules from the previous symbol. Similarly, the expected number of received MMs emitted in the current symbol duration, denoted

as $E[N_C^{Rx}]$, is $N \cdot F_{hit}(t_s, \lambda \mid r, d, D)$ for symbol "1", and 0 for symbol "0".

There are only two possible symbol sequences, which are "0" and "1". When k previous symbols are taken into consideration, the reception probabilities are calculated for each possible previous symbol sequence and then added in order to find the correct or erroneous demodulation probabilities as shown below:

$$
\begin{aligned}
P_{c_1} &= \sum_{i=1}^{2^k} p((E[N_{P_t}^{Rx}(S_i)] + E[N_C^{Rx}]) \geq \tau) \cdot p(S_i) \\
P_{c_0} &= \sum_{i=1}^{2^k} p(E[N_{P_t}^{Rx}(S_i)] < \tau) \cdot p(S_i) \\
P_{e_1} &= \sum_{i=1}^{2^k} p((E[N_{P_t}^{Rx}(S_i)] + E[N_C^{Rx}]) < \tau) \cdot p(S_i) \\
P_{e_0} &= \sum_{i=1}^{2^k} p(E[N_{P_t}^{Rx}(S_i)] \geq \tau) \cdot p(S_i)
\end{aligned} \tag{3.22}
$$

where S_i is the i^{th} possible symbol sequence, and $E[N_{P_t}^{Rx}(S_i)]$ is the total number of received molecules from previous symbols regarding S_i and calculated in a similar manner to $E[N_P^{Rx}]$. For all previous symbol values, the expected number of interference molecules are calculated and added.

In this thesis, we assume that sending "0" and "1" are equiprobable with $p = 0.5$, so each $p(S_i)$ is equal to $\frac{1}{2^k}$. As stated in [24], we consider the stray molecules only from four symbol durations before and we set $k = 4$.

4. ANALYSIS OF THE EFFECTS OF NON-ENZYMATIC DEGRADATION BY SIMULATIONS

In a 3D environment, traditional CvD system is compared to the CvD system utilizing MM degradation in the sense of molecule hitting times, ISI, detection performance, and mutual information [13]. The results clearly demonstrate that the degradation of MMs leads to a decrease in the ISI and the hitting time to the receiver NeN, while increasing the detection performance and the mutual information.

For each simulation scenario, in order to have a thorough analysis, we transfer 10,000 bits between the transmitter and the receiver NeN. Table 4.1 summarizes the parameters and their value ranges used in the simulations. Diffusion coefficient value is calculated according to the formulas given in Section 3.1 using the related parameter values stated below. Wide ranges of MM half-life values are considered for pointing out the difference in results clearly. The shortest distance from the surface of the receiver NeN to the point source is given as parameter d. Lastly, the step size of the movements of the MMs is chosen as 10^{-3} seconds in our simulations.

4.1. Molecule Hitting Times

In CvD systems, MM hitting time to the receiver NeN is a chief source of information about the behaviour of the system. It describes the fraction of molecules that arrive at the receiver NeN in a given time frame, over the total number of arriving molecules. With the usage of degrading MMs, the hitting time graph is expected to shift to the left since so-called *stray molecules* are eliminated due to degradation in time.

In Figure 4.1, we observe that the systems with increasing rate of degradation reach their respective equilibrium points faster and leave less stray molecules than sys-

Table 4.1. Simulation Parameters.

Parameter	**Value**
Number of MMs (N)	1000 - 6000
Liquid Viscosity (η)	0.001 $kg/(sec \cdot m)$
Stoke's radius of MMs (r_{MM})	$2.56 \cdot 10^{-9} m$
NeN Radius (r_{NeN})	10 μm
Absolute Temperature (T)	310 °K
Diffusion Coefficient (D)	79.4 $(\mu m)^2/sec$
MM Half-life ($t_{1/2}$)	16 - 2048 $msec$
Symbol Duration (t_s)	20 - 300 $msec$
Detection Threshold (τ)	1 - N
Distance to the Receiver NeN (d)	2 - 8 μm
Simulation Step Size (Δt)	1 $msec$

tems with lower rates of degradation. Notice that in the figure, where $d = 4\,\mu m$, the system with $t_{1/2} = 16 msec$ has no more stray molecules left in the channel after approximately 0.23 seconds and reaches the equilibrium point, whereas without degradation, 50% of the molecules remain in the channel at $t = 0.13$ seconds. This equilibrium for no degradation case may never be reached since there is always a chance of a molecule to arrive at the receiver even after a significant amount of time. Therefore, communication systems with no degradation approximate this equilibrium by defining a maximum fraction of arriving molecules.

4.2. Intersymbol Interference (ISI)

As mentioned before, ISI may lead to the erroneous demodulation of the information resulting from the arrival of the stray molecules left from previous symbol durations. The stray molecules arrive at the receiver NeN beyond the intended symbol duration. For instance, when the intended symbol is "0", according to our modulation technique, the transmitter NeN does not emit any molecules into the environment.

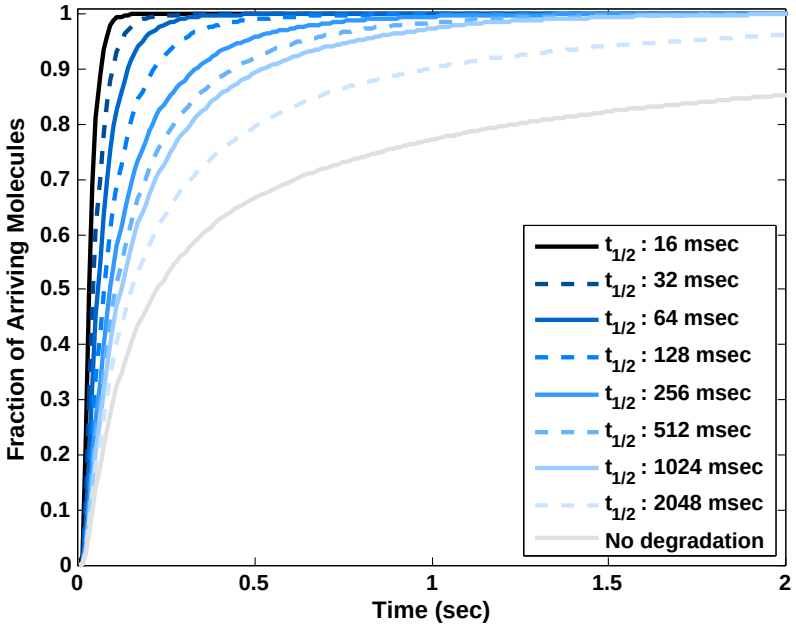

Figure 4.1. Fraction of arriving molecules for following symbol durations after a release.

However, the number of received molecules may exceed the threshold due to the stray molecules, and results in the incorrect demodulation of the symbol as "1". The communication impairments in CvD systems are generally caused by high ISI. Addition of MM degradation to the system works as a cleaning mechanism, which reduces the amount of residual MMs left from the previous symbol durations.

Figure 4.2 represents the fraction of molecules received in each symbol duration for four symbol durations, when t_s is 60 $msec$ and d is 4 μm. We did not continue after the fourth symbol duration since the number of stray molecules dramatically decreases and the simulations are elongated [24]. It can be easily observed that for higher rates of degradation, ISI in the system is significantly smaller compared to lower rates or no degradation systems. For no degradation case, the number of MMs arriving in the first symbol duration is nearly equivalent to the number of MMs arriving in the second symbol duration. On the other hand, in the cases where degradation is utilized, the difference in the number of molecules between the consecutive symbol durations increases as the degradation rate gets higher.

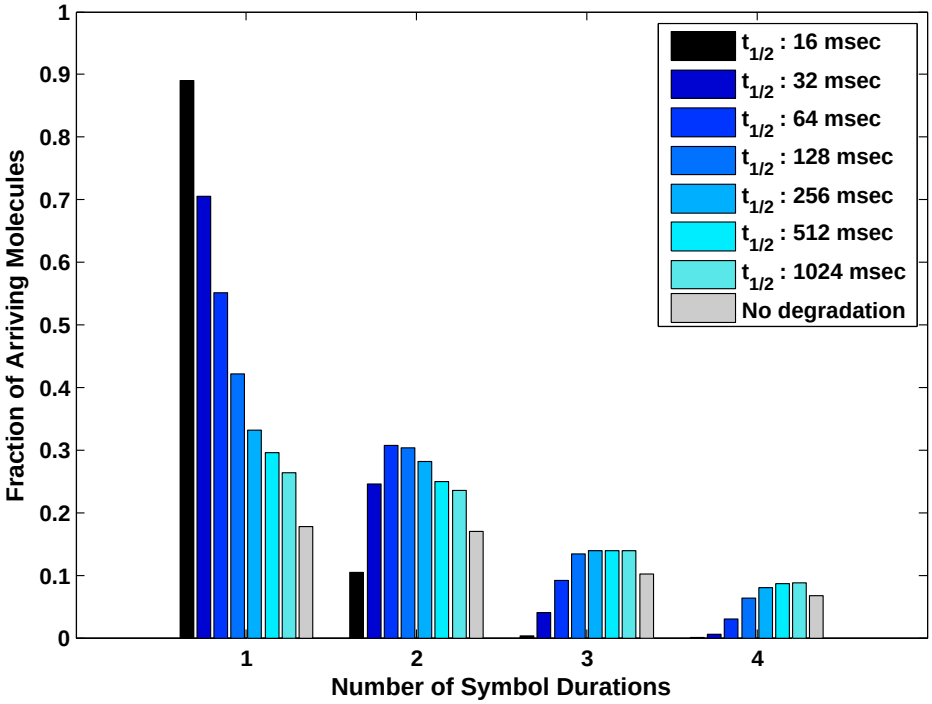

Figure 4.2. Hitting time histograms for various $t_{1/2}$ values.

4.3. Detection Performance

The reliability of the communication depends on the detection performance of the overall system. In our CvD system, the information demodulated in the receiver NeN is compared to the modulated information, i.e. intended symbol, for the calculation of the correct and false detection probabilities. The parameters P_{c_1} and P_{c_0} are calculated in the simulations by dividing total number of correctly received bits to the total intended number of bits of that bit value.

Figure 4.3 demonstrates the performance analysis using a ROC-curve representation. The x-axis in the figure is the probability that the receiver NeN demodulates the MM wave incorrectly as "1", i.e. P_{e_0}, which is when the number of received MMs in a symbol duration exceeds τ while the information sent is "0". On the y-axis, the values of P_{c_1}, the probability that the receiver correctly demodulates "1", are shown.

The figure articulates that the systems with higher degradation rates perform better over lower rates. The upward shift in the figure indicates a better communication performance. When the half-life value is chosen as $16, 32$, or $64\,msec$, the system has nearly perfect performance, whereas the performance continually converges to base level with increasing $t_{1/2}$ values. The sooner the MMs degrade, the less chance they have of arriving late and causing ISI at the receiver. Therefore a shorter $t_{1/2}$ duration results in a higher correct detection probability.

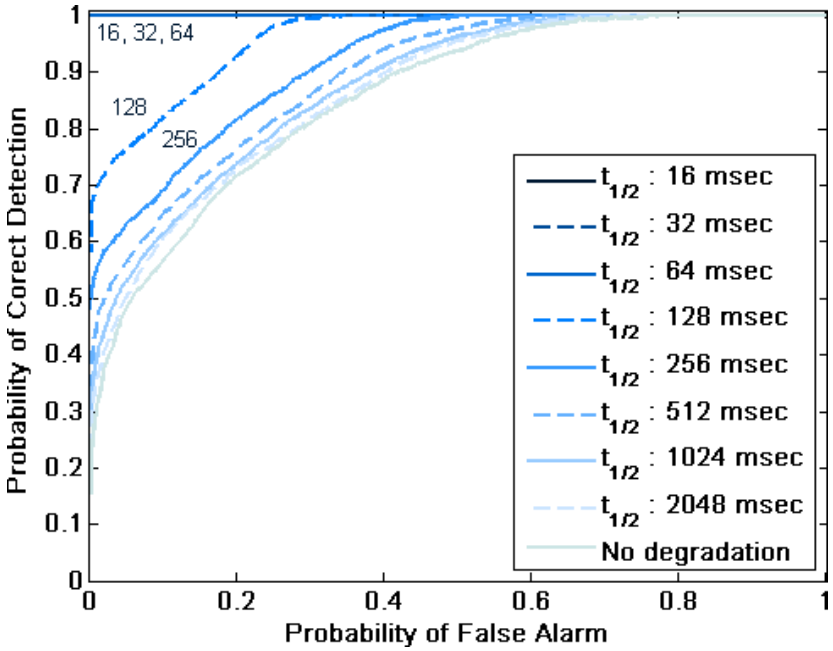

Figure 4.3. ROC curves for various $t_{1/2}$ values.

On the other hand, when the correct detection rate increases, the system is inclined to produce more false alarms. In order to achieve better detection of 1s, τ can be diminished. This way, the probability of the incorrect demodulation of "1" is prevented. However, this reduction in τ also affects the demodulation of "0", since some MMs released in the previous symbol durations may arrive in the current symbol duration. This results in the reception of non-expected molecules at the receiver side. A lower τ value may, therefore, result in the incorrect demodulation of "0" as "1" that causes an increase in the false alarm rate.

4.4. Mutual Information

Another metric that affects the communication is mutual information, which is described in Section 3.2.2. According to the simulation results shown in Figure 4.4, it is demonstrated that the threshold value (τ) that maximizes the mutual information decreases when the half-life value is smaller, i.e. degradation is faster. In the figure, distance between the NeNs is chosen as 4 μm, while the symbol duration is 60 $msec$. The decrease in the threshold values is not surprising since the number of MMs reaching at the receiver decreases when the degradation is fast.

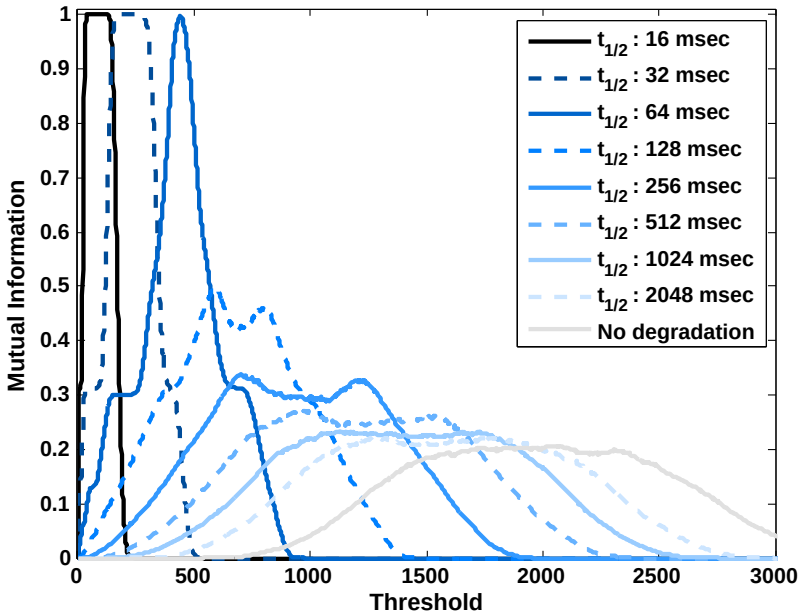

Figure 4.4. Mutual information in the channel vs. the corresponding threshold values for different $t_{1/2}$ values.

5. PARAMETER VALUE SELECTION FOR CORRECT DEMODULATION OF THE SIGNAL

In this chapter, we introduce two boundary conditions for a robust and a reliable CvD system. First one is $P_r(t, \lambda \mid r_{NeN}, d, D) > \frac{\tau}{N}$ in order to be able to correctly detect "1". Since we use BCSK as the modulation technique, the receiver demodulates the signal as "1" only when the number of received molecules in the corresponding symbol duration exceeds the predefined threshold value. The other boundary condition is $P_s(N, t, \lambda \mid r_{NeN}, d, D) < \frac{\tau}{N}$ to avoid the incorrect demodulation of the MM signal. Using this boundary, ISI caused by the stray molecules remaining from the previous symbol duration is eliminated.

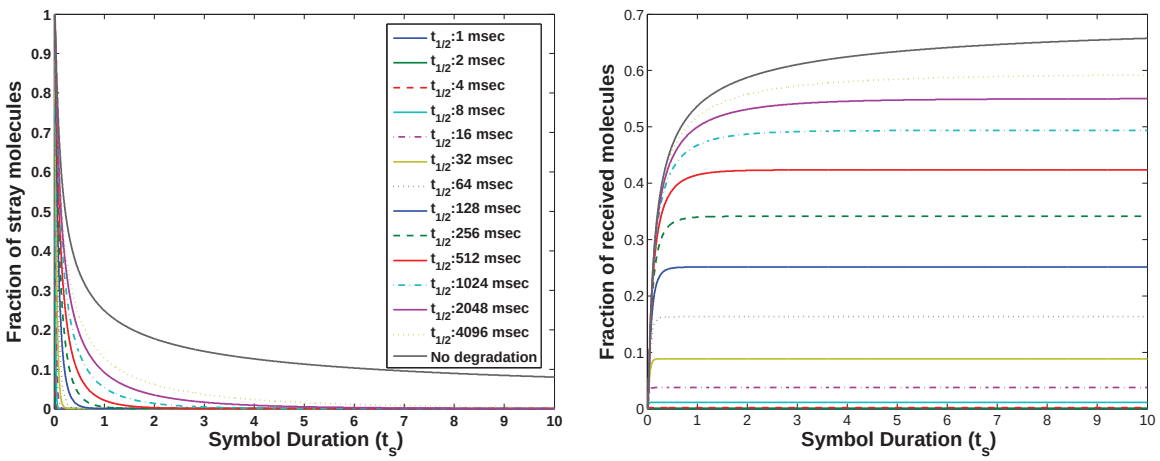

Figure 5.1. Change in the fraction of stray and received molecules with increasing symbol duration values when $d = 4\mu m$.

In this sense, we use the analytical expressions given in Section 3.3 in the calculation of the number of received and stray molecules. Figure 5.1 shows the effect of symbol duration and the MM degradation half-life on these probabilities. As expected, for any half-life value, fraction of stray molecules decrease with increasing symbol duration values, while fraction of received molecules increase. In addition, the curves in the left are convex where they are concave for the right figure.

When the boundary conditions are considered, the parameter values for $\frac{\tau}{N}, t_s$, and $t_{1/2}$ are restricted. That is, for some combinations of the values of these parameters, $P_r(t, \lambda \mid r_{NeN}, d, D)$ is never greater or $P_s(N, t, \lambda \mid r_{NeN}, d, D)$ is never smaller than $\frac{\tau}{N}$. In the following sections, we focus on the selection of the values for aforementioned parameters assuring the boundary conditions.

5.1. Symbol Duration Selection

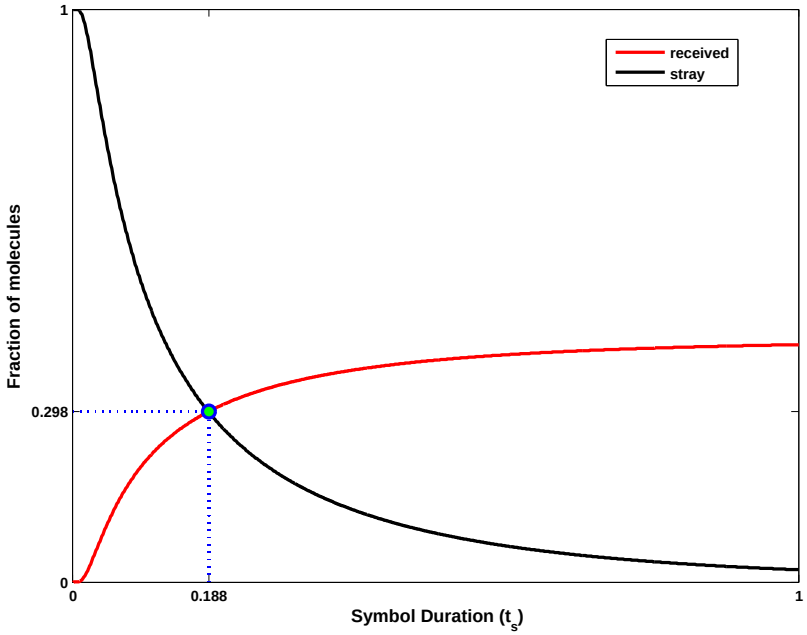

Figure 5.2. The fraction of stray and received molecules when $d = 4\mu m, t_{1/2} = 512$ msec and $N = 10000$ molecules.

The boundary conditions are also affected by the value of symbol duration. For a given parameter value combination, there is a set of appropriate selections of symbol duration values to achieve the attempted goals. Figure 5.2 demonstrates the change in the fraction of received and stray molecules with symbol duration when the distance between the communication pair is $4\mu m$ and the MM degradation half-life is set to 512 msec. As shown in the previous figures also, these fraction curves behave conversely with respect to symbol duration. Thus, two curves intersect at a point that assures the boundary conditions.

In Figure 5.2, the symbol duration value of the intersection point shows the minimum t_s value that the boundary conditions can be achieved. That is, for the corresponding setup, if the symbol duration is selected less than 188 msec, for any threshold value neither of the conditions is accomplished.

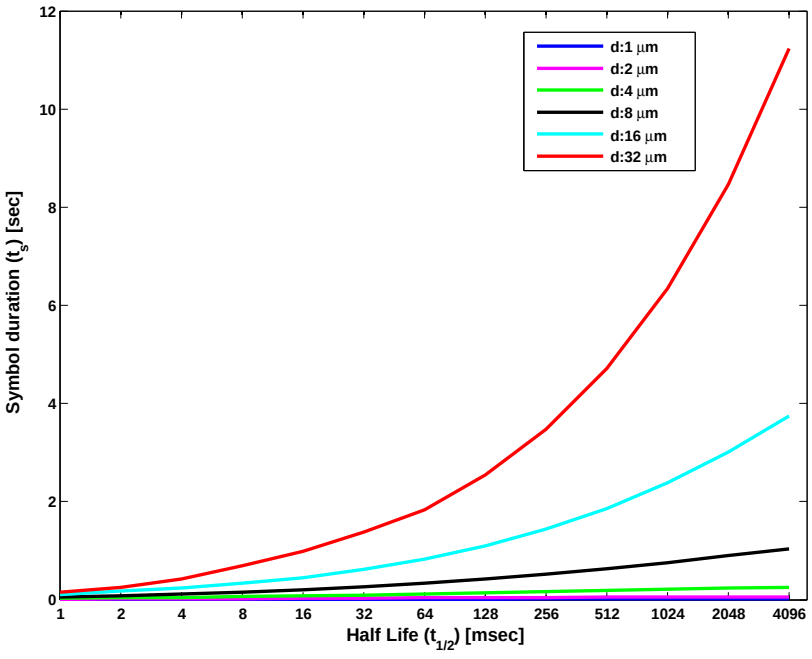

Figure 5.3. The minimum required symbol duration values assuring the boundary conditions with respect to degradation half-life and distance.

Figure 5.3 shows the effect of degradation on the aforementioned minimum symbol duration values. When a fast degrading MM is utilized in the communication, this minimum duration value decreases independent of distance. The positive effect is more apparent at longer distances. When the distance between the transmitter and the receiver is set to $32\mu m$, the obtained symbol duration values range from 155 msec to approximately 11 sec.

Choosing the minimum among all possible symbol duration values is beneficial especially in terms of data rate increment. As depicted in Equation 3.9, the shorter the symbol duration, the higher the data rate. According to the results shown in Figure 5.3, utilizing degradation in CvD systems helps to achieve more reliable systems. This

effect is investigated further in the next chapter.

5.2. Threshold Selection

There are two boundary conditions that we aim in this chapter. One of them is to receive less stray molecules that the threshold value. As seen in Figure 5.1, when degradation is considered, the fraction of stray molecule curves arrives at the x-axis. This does not happen in this figure only for the case that the MMs are excepted to never degrade. Thus, choosing the appropriate symbol duration value we are able to stay within the desired limits.

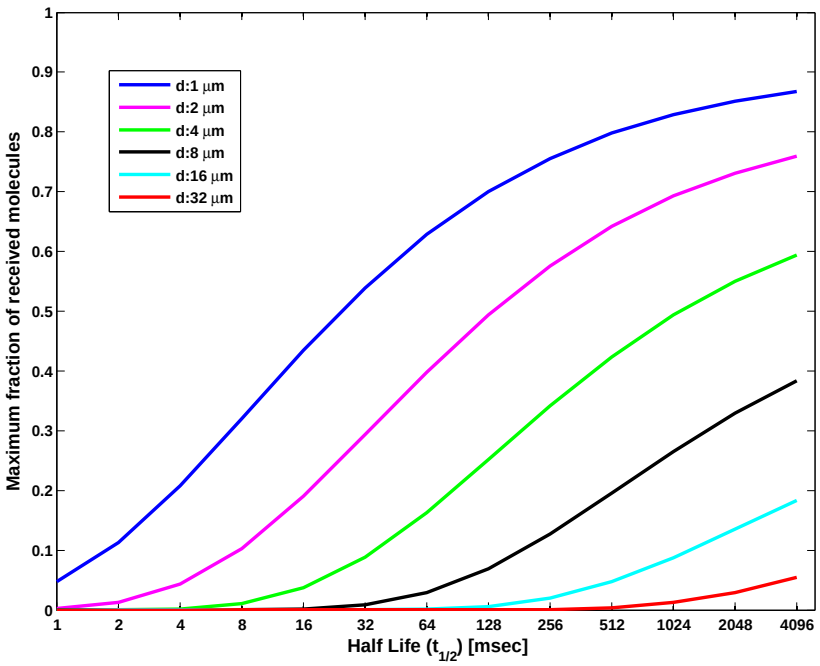

Figure 5.4. The maximum fraction of received molecules for different degradation half-life and distance values.

Regarding the other limitation, which is $P_r(t, \lambda \mid r_{NeN}, d, D) > \frac{\tau}{N}$, we see that the degradation utilizing system curves for the fraction of the received molecules in Figure 5.1 converges to a specific point. Especially for fast degrading MMs, the maximum of these values are very small. This property limits the threshold selection up to the

above-referred values.

Figure 5.4 demonstrates the change in these maximum values with respect to MM degradation half-life and distance. When a fast degrading molecule is utilized in the communication environment, a very small portion of the released molecules is expected to be received by the receiver NeN within the corresponding symbol duration. On the other hand, the increase in the distance between the transmission couple effects this portion negatively. That is, for longer distances, the maximum achievable fraction of received molecules are less than shorter ones.

5.3. Degradation Half-Life Selection

As stated in the previous parts, distance and the MM degradation half-life affect the fraction of received and stray molecules in CvD systems. Especially when the received MM fraction is concerned, some $(d, t_{1/2})$ combinations may lead to very small reception rate as seen in Figure 5.4.

Assume that the transmitter releases 1000 molecules for symbol "1" ($N = 1000$). These molecules, when emitted $8\mu m$ away from the receiver, are expected to be received with 4.0928×10^{-6} probability if the half-life value is 4 milliseconds. In this case, the expected number of received molecules will be 4.0928×10^{-3} since the probability is multiplied with the number of transmitted molecules. Although we calculate the probabilities continuously, our CvD system demodulates the signal discretely. Thus, as shown in this example scenario, some half-life values can be inappropriate for some systems.

Figure 5.5 demonstrates the appropriate half-life values for distances from 1 to $32\mu m$. In this representation, we show also the effect of number of released molecules on the half-life selection. According to the results, emission of more molecules leads to an increase in the range of the appropriate MM degradation half-life values. This effect is more apparent at longer distances due to the dramatical decrease in the fraction of the received molecules. In addition, this decrease causes the half-life value band to be

narrow for each N selection.

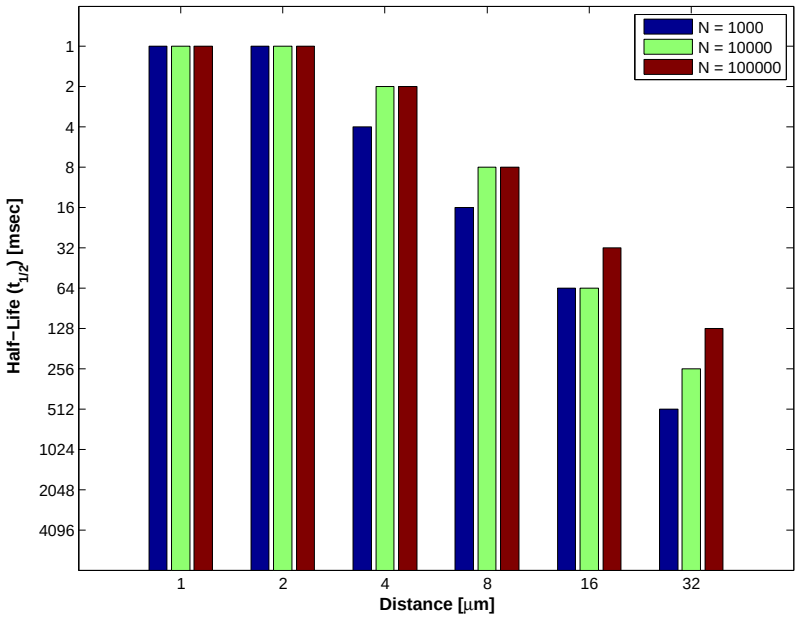

Figure 5.5. The half-life values appropriate to utilize in different distances and corresponding N values.

6. EFFECTS ON THE DATA RATE AND THE ENERGY CONSUMPTION

One of the most important metrics of a communication system is the data rate. As explained in Section 3.2.2, this metric depends on the detection probabilities, channel capacity, and the symbol duration. Higher data rates correspond to more reliable systems. Therefore, we investigate the effects of degradation concept on 3D CvD systems comparing with the systems that ignore this concept.

While mitigating ISI and increasing the data rate of the system, we need to consider also the energy expenditure. The system with less energy cost would be more applicable in handling the communication. Since MM production requires energy, minimizing the total number of emitted molecules (N) results in less energy consumption as depicted in Section 3.2.3. However, for smaller values of N, the data rate of the system decreases. So, the values of the communication parameters should be chosen correctly in order to balance energy expenditure and the improvements in communication.

Using the analytical formulas explained Section 3.3, we compute the data rate of the overall system and the energy expenditure of the transmitter for different half-life values and compare the results with a system in which degradation is not considered.

6.1. Data Rate Gain

The data rate of the system depends on the channel capacity and the symbol duration values as shown in Equation 3.9. The channel capacity increases when more MMs are emitted. Thus, the transmitter needs to spend more energy in order to accomplish higher data rates. In order to express the effect of molecule degradation on data rate, we calculate (N, t_s) pair for each distance that acquires a high percentage of the maximum achievable data rate for the case when degradation is not considered. Then, we compare the obtained data rate values for the cases utilizing MM degradation

using the same (N, t_s) pair.

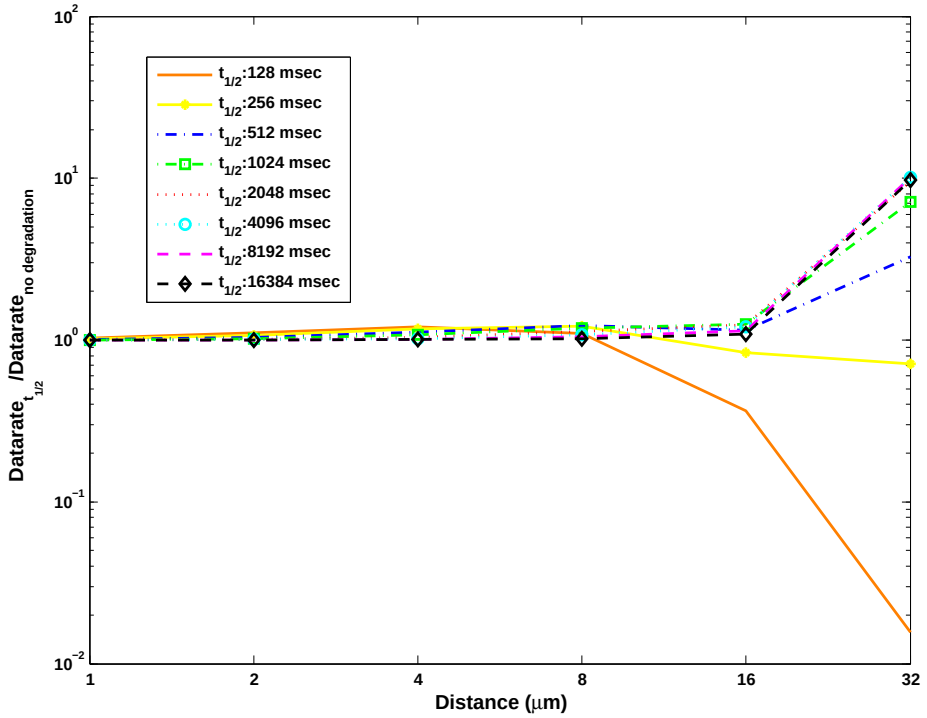

Figure 6.1. The ratio of data rate values in the no-degradation case and to the cases utilizing degradation with half-life values ranging from 128 msec to 16.384 sec.

In Figure 6.1, there is a slight gain in the data rate for all half-life values up to $8\mu m$. This gain increases in longer distances when the MM half-life is selected greater than or equal to 512 msec. However, the obtained data rate becomes smaller compared to the no-degradation case for lower half-life values, since within the corresponding symbol durations most of the MMs get degraded. Especially for the case that MM degradation half-life is 128 msec, there is a sharp decrease in the data rate when the distance between the transmitter and the receiver is long.

Figure 6.2 indicates that the usage of small half-life values in our MCvD model results in lower data rate compared to the no-degradation case. When the same amount of MMs are emitted, the systems with half-life values ranging from 1 msec to 64 msec perform worse due to the fast degradation of the information carrying molecules. For

small degradation half-lives, the overall data rate of the system decreases so dramatically that some of the curves in the figure cannot go beyond longer distances. For instance, when the distance is more than 4 μm, the data rate is nearly zero for half-lives of 1 and 2 msec.

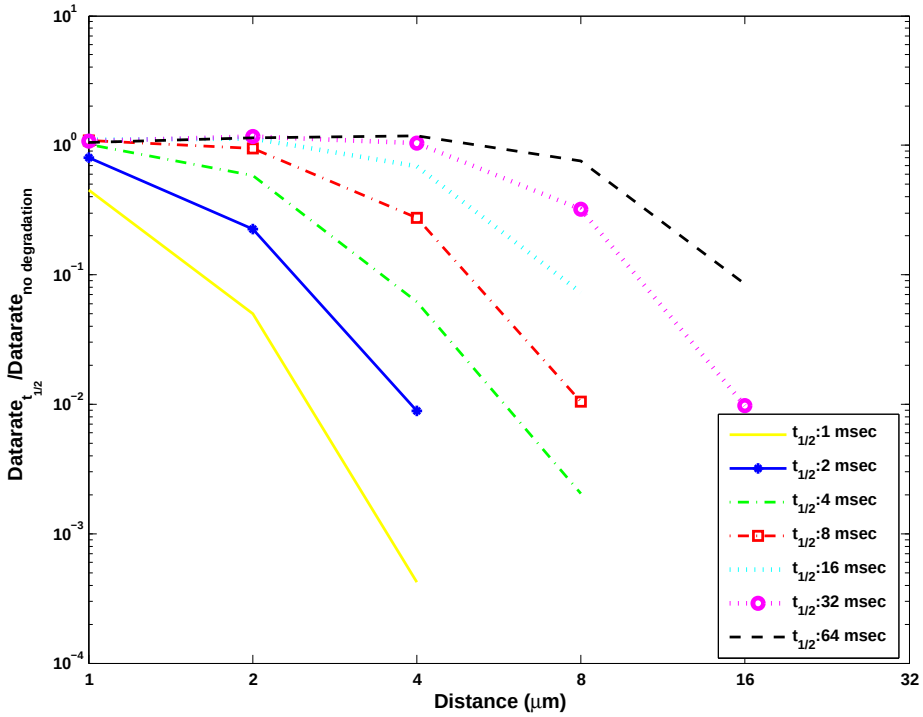

Figure 6.2. The ratio of the data rate values in the no-degradation case and to the cases utilizing degradation with half-life values ranging from 1 msec to 64 msec.

6.2. Decrease in the Energy Consumption

In this section, we reckon the energy consumed for the transmission of the information as directly proportional to the number of MMs. Thus, we decrease the energy consumption when the transmitter emits fewer MMs. Here, we calculate the optimal symbol duration value that maximizes the data rate for distances 1 μm to 32 μm and $N = 100,000$ molecules when degradation is not utilized. Then, we compute the required number of molecules to accomplish the same data rate using the same symbol duration values for the cases where different half-life values are selected.

In Figure 6.3, the comparison is shown when the half-life values are chosen between 256 msec and 16,384 msec. Intuitively, the systems utilizing degradation is expected to emit more molecules in order to achieve the same data rate as the no-degradation case, since the number of MMs decrease in time. However, the figure shows that utilizing degradation in MCvD decreases the energy consumption, since all curves stay above 1 when $t_{1/2}$ values are selected between 128 and 16,384 msec. This happens due to the decrease in ISI and increase in the mutual information. The optimal half-life value for a specific distance is correlated with the symbol duration selection for that distance. For instance, for $d = 4\mu m$, the symbol duration value that maximizes the data rate for no-degradation case is 113 msec while the maximum ratio on the y-axis is achieved when the half-life is chosen as 128 msec.

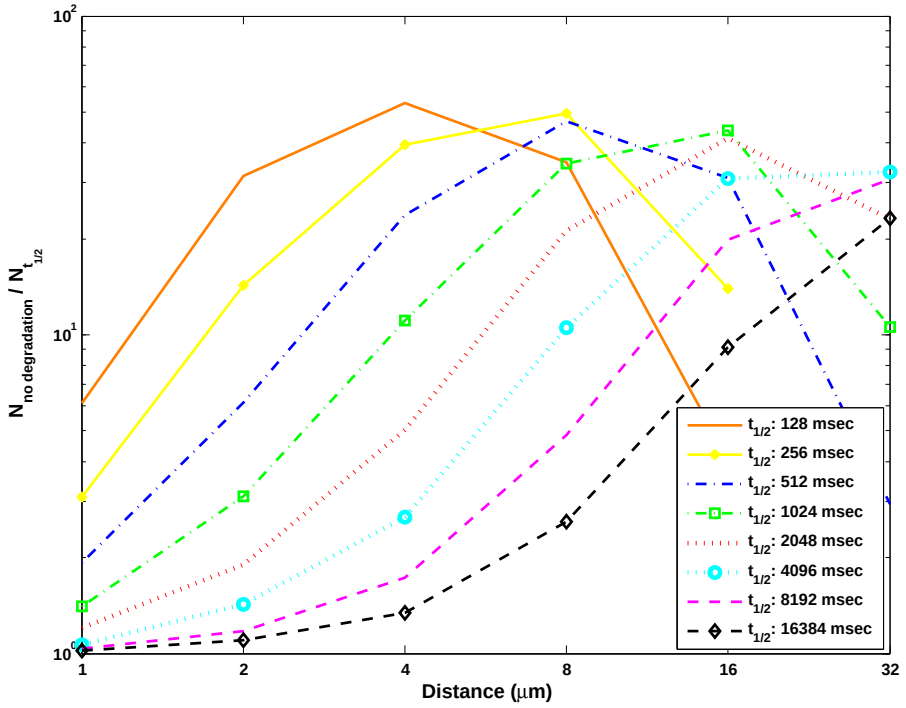

Figure 6.3. The ratio of the number of emitted molecules in the no-degradation case and to the cases utilizing degradation with half-life values ranging from 128 msec to 16.384 sec.

Figure 6.4 shows the ratios of the number of MMs transmitted when small half-life values are chosen. Especially for short distances, choosing these values decreases

the energy expenditure. However, they do not provide any connectivity at all for longer distances. Since the MMs degrade in a very fast manner, they cannot arrive at the receiver that decreases the number of received MMs. When the half-life value is selected as 4 msec, for instance, the target data rate for distances longer than 4 μm cannot be achieved even when excessive number of molecules are emitted.

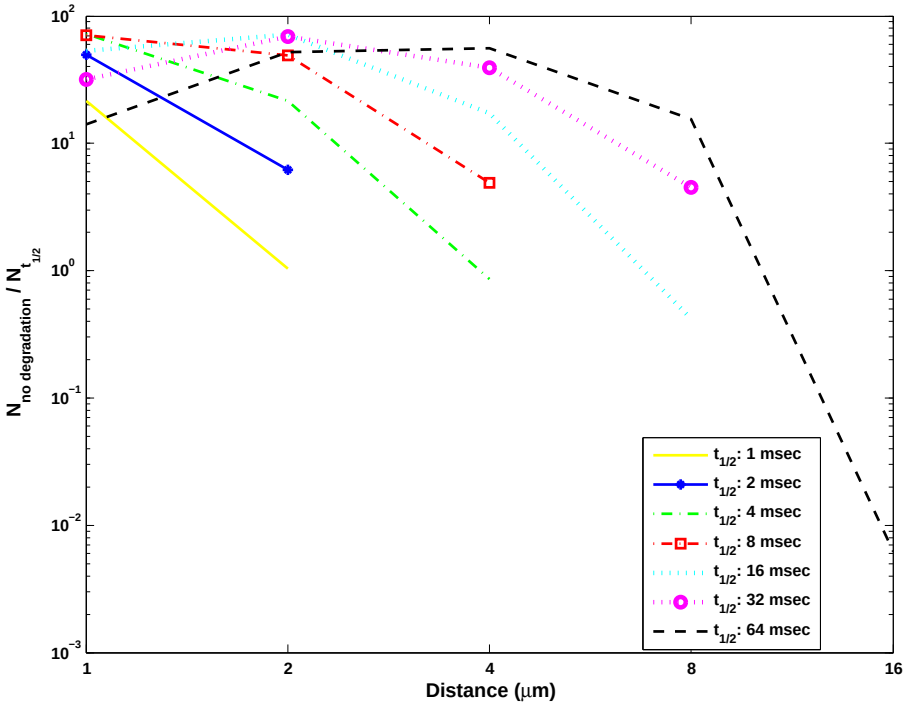

Figure 6.4. The ratio of the number of emitted molecules in the no-degradation case and to the cases utilizing degradation with half-life values ranging from 1 msec to 64 msec.

7. CONCLUSIONS AND FUTURE DIRECTIONS

Being a relatively new system, Communication via Diffusion is studied by many researchers. There are several works considering the basic signaling issues and high level mechanisms. Common problems of this communication system can be listed as high Intersymbol Interference, low symbol detection probabilities, and low channel capacities. In this thesis, we elaborate on MM degradation in 3D CvD systems in order to overcome these considerations.

We cover the degradation concept via both simulating the scenario and making use of analytical expressions. We demonstrate the effects of degradation on molecule hitting times, ISI, detection performance, and mutual information with simulations. The results show that using degradation to our advantage plays a crucial role in decreasing stray molecules. A very large percentage of messenger molecules that arrive at the receiver do arrive when they are supposed to, instead of being stray molecules that affect the successor symbols. Precisely, we show that MM degradation increases the communication accuracy in the channel by reducing ISI. Additionally, we show that the false alarm rate is greatly reduced with shorter MM half-life, while the mutual information is increased.

Using the analytical formulas of the reception and straying probabilities, we select the values for communication parameters in order to increase the probability of correctly demodulating the signal. We calculate the appropriate symbol duration, threshold, and MM degradation half-life values for different communication setups. When degradation is utilized, we show that the minimum required symbol durations assuring the boundary conditions increase with longer distances and slower degradation rate. However, CvD systems with shorter MM half-lives results in a decrease in the maximum reception rate especially in longer distances. On the other hand, we propose the appropriate half-life value ranges for different distance and number of released molecules.

In this thesis, we also work on the basic needs of the communication environment. Our aim is to increase the data rate and reduce the energy consumption. In this sense, we represent the effects of the values of the aforementioned communication parameters on these concepts. According to the results, we ascertain that the proper usage of degradation improves the communication performance. Due to the decrease in the ISI, the transmission energy reduces while the channel capacity, and thus, the data rate of the system increase. Precisely, we obtain an energy efficient and accurate model by utilizing MM degradation in MCvD. When the energy expenditure is considered, the systems utilizing degradation performs better over the system ignoring MM degradation. Additionally, when the MM half-life values are selected carefully, the obtained data rate slightly increases regarding the data rate of the no-degradation case.

As future work, we plan to work on the effects of the other communication parameters, such as the diffusion coefficient and the radius of the receiver, on the communication. Besides these parameters, the total study can be replicated using a different modulation technique or different boundary conditions. We also plan to focus on enzymatic degradation in our CvD model and compare its results with non-enzymatic degradation. In addition, extending our system to a multi-user environment is another future continuation of this thesis.

APPENDIX A: HISTORY OF BROWNIAN MOTION

Although it is named after Robert Brown, it was Jan Ingenhousz who first discovered that random motion as "fluctuating movements of carbon dust particles in alcohol" [46]. However, he failed to describe the motion correctly. In 1827, nearly after a half century, Robert Brown published a paper about Brownian motion, which is described as the motion of pollens in water [41]. He explained the stochastic movements of small particles suspended in a solution as being chaotic and non-directed while being governed by the combination of forces applied by the molecules composing the solution as depicted in Figure A.1. In the very same year, Adolphe Brongniart also made similar observations of these movements [47].

Before the botanist Robert Brown, these movements were thought to be caused by only living organisms. It was Brown who showed that inorganic pollen grains in the suspension also had an irregular motion. Starting point of the implications of Brownian motion among the scientists such as Jean Baptiste Perrin [48], Albert Einstein [49], Marian Smoluchowski [50], and many others, has its roots in the publications of Leon Gouy in 1880s. He showed Brownian motion as a fundamental physical property of fluid matter. In his experiments, Gouy convinced that Brownian motion had demonstrated

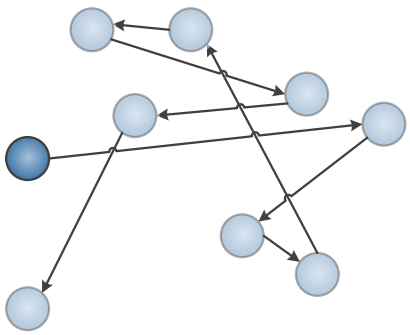

Figure A.1. Brownian movement of a molecule.

the statistical nature of the laws of thermodynamics in reality by proposing the "non-absoluteness" of the second law of thermodynamics at microscopic scales [51].

In addition, Regarding the molecular-kinetic theory, Einstein was demonstrating the contradiction between Brownian motion theory and classical thermodynamics by arguing the existence of 'colloidal osmotic pressure' [49]. In the following measurements and comprehensive researches, Brownian motion is modeled by various scientist with respect to fluid dynamics.

In the liquid environment, molecule dissipation is described by the diffusion parameters. The diffusion model is based on Fick's law, which states that the flux goes from the high concentration to low [52]. Inspired from the Fick's law, in their independent works, Einstein and Smoluchowski combine the connection between the fluid dynamics and the diffusion as *Einstein-Smoluchowski relation*. This relation defines one of the most important parameters of diffusion: *diffusion coefficient*. This coefficient, denoted by D, describes the likeliness of the propagation of the molecule through the fluid environment [53]. It is calculated as

$$D = \mu k_B T \tag{A.1}$$

where k_B is the Boltzmann constant, T is the absolute temperature, and μ is the mobility. For higher values of D, molecules diffuse faster. For biological molecules, the diffusion coefficient has a range from 10^{-11} to $10^{-10} m^2/sec$.

An important form of the Einstein-Smoluchowski relation is *Stokes-Einstein equation*. This equation demonstrates the importance of the sizes of the liquid molecules and the diffusing ones. It defines the frictional coefficient (or the drag coefficient) ζ, which is the inverse of μ, to incorporate the slipperiness of the molecules among the liquid molecules, and calculated as

$$\zeta = 6\pi\eta r \tag{A.2}$$

where η is the viscosity of the liquid and r is *Stoke's radius*, which is defined as the radius of a sphere whose diffusive properties in the same communication environment is identical to those of MMs'. According to *Stoke's law*, Equation A.2 is valid when the size of the propagating molecule is much greater compared to the size of the liquid molecules and the viscous forces are dominant in the flow [54]. In this case, Reynold's number, which is the ratio of inertial forces to viscous forces in the fluid, is low. In [55], it is shown that the frictional coefficient reduces to

$$\zeta = 4\pi\eta r \tag{A.3}$$

when the Reynold's number is high as in turbulent flows.

APPENDIX B: DERIVATION OF MUTUAL INFORMATION FORMULAS

As shown in Equation 3.3, the mutual information is expressed as:

$$I(X;Y) \;=\; \sum_{y\in Y}\sum_{x\in X} p(x,y)\log_2\left(\frac{p(x,y)}{p(x)p(y)}\right) \tag{B.1}$$

Since $X, Y \in \{0,1\}$, we can represent the above summation as:

$$\begin{aligned} I(X;Y) \;=& p(x=0,y=0)\,log_2\left(\frac{p(x=0,y=0)}{p(x=0)\,p(y=0)}\right)+ \\ & p(x=0,y=1)\,log_2\left(\frac{p(x=0,y=1)}{p(x=0)\,p(y=1)}\right)+ \\ & p(x=1,y=0)\,log_2\left(\frac{p(x=1,y=0)}{p(x=1)\,p(y=0)}\right)+ \\ & p(x=1,y=1)\,log_2\left(\frac{p(x=1,y=1)}{p(x=1)\,p(y=1)}\right) \end{aligned} \tag{B.2}$$

We assume that sending symbol "0" and "1" are equiprobable with 0.5. Also, we define the received symbol probabilities in Equations 3.4 and 3.5. In addition, we use the Bayes' theorem in defining the joint probabilities, which states that:

$$p(x,y) \;=\; p(y \mid x)\,p(x) \tag{B.3}$$

where, in our case, the conditional probabilities ($p(y=0 \mid x=0)$, $p(y=1 \mid x=1)$, $p(y=1 \mid x=0)$, $p(y=0 \mid x=1)$) are P_{c_0}, P_{c_1}, P_{e_0}, and P_{e_1}, respectively. Thus,

we rewrite the reception probabilities as:

$$I(X;Y) = \frac{1}{2}\left\{P_{c_0}\log_2\left(\frac{2P_{c_0}}{P_{c_0}+P_{e_1}}\right)+P_{e_0}\log_2\left(\frac{2P_{e_0}}{P_{e_0}+P_{c_1}}\right)+ P_{c_1}\log_2\left(\frac{2P_{c_1}}{P_{c_1}+P_{e_0}}\right)+P_{e_1}\log_2\left(\frac{2P_{e_1}}{P_{e_1}+P_{c_0}}\right)\right\} \quad \text{(B.4)}$$

which is the mutual information formula given in Equation 3.6. Moreover, we use the multiplication and division properties of logarithms stating that:

$$log\left(\frac{a}{b}\right) = log(a) - log(b)\ ,\ log(a\cdot b) = log(a) + log(b) \quad \text{(B.5)}$$

which are independent of the base of the logarithm. Using these properties, the logarithms in Equation 3.6 is simplified and the equation becomes:

$$\begin{aligned} I(X;Y) = \frac{1}{2}\{\, & P_{c_0}[1+\log_2(P_{c_0})+\log_2(P_{c_0}+P_{e_1})]+ \\ & P_{e_0}[1+\log_2(P_{e_0})+\log_2(P_{e_0}+P_{c_1})]+ \\ & P_{c_1}[1+\log_2(P_{c_1})+\log_2(P_{c_1}+P_{e_0})]+ \\ & P_{e_1}[1+\log_2(P_{e_1})+\log_2(P_{e_1}+P_{c_0})]\} \end{aligned} \quad \text{(B.6)}$$

The last step to obtain the formula in Equation 3.7 is to apply the facts that $P_{c_1}+P_{e_1} = 1$ and $P_{c_0}+P_{e_0} = 1$. Then, these probabilities are summed up to 2. When the common factors ($\log_2(P_{c_0}+P_{e_1})$ and $\log_2(P_{e_0}+P_{c_1})$) are combined, the formula becomes:

$$\begin{aligned} I(X;Y) = \frac{1}{2}[\, & 2 + P_{c_0}\log_2(P_{c_0}) + P_{e_0}\log_2(P_{e_0}) + P_{c_1}\log_2(P_{c_1}) + P_{e_1}\log_2(P_{e_1}) \\ & -(P_{c_0}+P_{e_1})\log_2(P_{c_0}+P_{e_1}) - (P_{e_0}+P_{c_1})\log_2(P_{e_0}+P_{c_1})] \end{aligned} \quad \text{(B.7)}$$

REFERENCES

1. Moore, G. E., "Cramming More Components onto Integrated Circuits", Vol. 38, pp. 114 – 117, 1965.

2. Dubash, M., "Moore's Law Is Dead, Says Gordon Moore", *Techworld (April 2005)*, 2005.

3. Prasad, S. K., *Modern Concepts in Nanotechnology*, Vol. 5, Discovery Publishing House, 2008.

4. Akyildiz, I. F., F. Brunetti and C. Blázquez, "Nanonetworks: A New Communication Paradigm", *Computer Networks*, Vol. 52, No. 12, pp. 2260–2279, 2008.

5. Akyildiz, I. F., J. M. Jornet and M. Pierobon, "Nanonetworks: A New Frontier in Communications", *Communications of the ACM*, Vol. 54, No. 11, pp. 84–89, 2011.

6. Hiyama, S., Y. Moritani, T. Suda, R. Egashira, A. Enomoto, M. Moore and T. Nakano, "Molecular Communication", *Journal-Institute of Electronics Information and Communication Engineers*, Vol. 89, No. 2, p. 162, 2006.

7. Kuran, M. S., H. B. Yilmaz and T. Tugcu, "A Tunnel-Based Approach for Signal Shaping in Molecular Communication", *Communications Workshops (ICC), 2013 IEEE International Conference on*, pp. 776–781, IEEE, 2013.

8. Genc, G., H. B. Yilmaz and T. Tugcu, "Reception Enhancement with Protrusions in Communication via Diffusion", *Communications and Networking (BlackSeaCom), 2013 First International Black Sea Conference on*, pp. 89–93, IEEE, 2013.

9. Alberts, B., A. Johnson, J. Lewis, M. Raff, K. Roberts and P. Walter, *Molecular Biology of the Cell*, Garland Science, 2002.

10. Nakano, T., Y. Okaie and J. Q. Liu, "Channel Model and Capacity Analysis of Molecular Communication with Brownian Motion", *Communications Letters, IEEE*, Vol. 16, No. 6, pp. 797–800, 2012.

11. Arifler, D., "Capacity Analysis of a Diffusion-Based Short-Range Molecular Nano-Communication Channel", *Computer Networks*, Vol. 55, No. 6, pp. 1426–1434, 2011.

12. Noel, A., K. C. Cheung and R. Schober, "Using Dimensional Analysis to Assess Scalability and Accuracy in Molecular Communication", *Communications Workshops (ICC), 2013 IEEE International Conference on*, pp. 818–823, IEEE, 2013.

13. Heren, A. C., F. N. Kilicli, G. Genc and T. Tugcu, "Effect of Messenger Molecule Decomposition in Communication via Diffusion", *Nanoscale Computing and Communication (NANOCOM), 1st ACM International Conference on*, ACM, 2014.

14. Bush, S. F., *Nanoscale Communication Networks*, Artech House, 2010.

15. Piro, G., L. A. Grieco, G. Boggia and P. Camarda, "Simulating Wireless Nano Sensor Networks in the Ns-3 Platform", *Advanced Information Networking and Applications Workshops (WAINA), 2013 27th International Conference on*, pp. 67–74, IEEE, 2013.

16. Freitas, R. A., *Nanomedicine, Volume I: Basic Capabilities*, Landes Bioscience Georgetown, TX, 1999.

17. Akyildiz, I. F. and J. M. Jornet, "The Internet of Nano-Things", *Wireless Communications, IEEE*, Vol. 17, No. 6, pp. 58–63, 2010.

18. Jornet, J. M., "Low-Weight Channel Codes for Error Prevention in Electromagnetic Nanonetworks in the Terahertz Band", *Nanoscale Computing and Communication (NANOCOM), 1st ACM International Conference on*, ACM, 2014.

19. Jornet, J. M. and I. F. Akyildiz, "Channel Capacity of Electromagnetic Nanonetworks in the Terahertz Band", *Communications (ICC), 2010 IEEE International Conference on*, pp. 1–6, IEEE, 2010.

20. Kuran, M. S., H. B. Yilmaz, T. Tugcu and B. Ozerman, "Energy Model for Communication via Diffusion in Nanonetworks", *Nano Communication Networks*, Vol. 1, No. 2, pp. 86–95, 2010.

21. Garralda, N., I. Llatser, A. Cabellos-Aparicio and M. Pierobon, "Simulation-Based Evaluation of the Diffusion-Based Physical Channel in Molecular Nanonetworks", *Computer Communications Workshops (INFOCOM WKSHPS), 2011 IEEE Conference on*, pp. 443–448, IEEE, 2011.

22. Cooper, G. M. and R. E. Hausman, *The Cell*, Sinauer Associates Sunderland, 2000.

23. Gilbert, S. F., *Developmental Biology*, Sinauer Associates Sunderland (MA), 2000.

24. Kuran, M. S., H. B. Yilmaz, T. Tugcu and I. F. Akyildiz, "Interference Effects on Modulation Techniques in Diffusion Based Nanonetworks", *Nano Communication Networks*, Vol. 3, No. 1, pp. 65–73, 2012.

25. Moore, M. J., T. Suda and K. Oiwa, "Molecular Communication: Modeling Noise Effects on Information Rate", *NanoBioscience, IEEE Transactions on*, Vol. 8, No. 2, pp. 169–180, 2009.

26. Mahfuz, M. U., D. Makrakis and H. T. Mouftah, "Characterization of Intersymbol Interference in Concentration-Encoded Unicast Molecular Communication", *Electrical and Computer Engineering (CCECE), 2011 24th Canadian Conference on*, pp. 000164–000168, IEEE, 2011.

27. Lin, W. A., Y. C. Lee, P. C. Yeh and C. h. Lee, "Signal Detection and ISI Cancellation for Quantity-Based Amplitude Modulation in Diffusion-Based Molecular Communications", *Global Communications Conference (GLOBECOM), 2012*

IEEE, pp. 4362–4367, IEEE, 2012.

28. Yilmaz, H. B., N. R. Kim and C. B. Chae, "Effect of ISI Mitigation on Modulation Techniques in Communication via Diffusion", *arXiv preprint arXiv:1401.3410*, 2014.

29. Noel, A., K. C. Cheung and R. Schober, "Improving Diffusion-Based Molecular Communication with Unanchored Enzymes", *arXiv preprint arXiv:1305.1783*, 2013.

30. Tangpasuthadol, V., S. M. Pendharkar and J. Kohn, "Hydrolytic Degradation of Tyrosine-Derived Polycarbonates, a Class of New Biomaterials. Part I: Study of Model Compounds", *Biomaterials*, Vol. 21, No. 23, pp. 2371–2378, 2000.

31. Brunton, L. L., J. S. Lazo and K. L. Parker, *Goodman and Gilman's the Pharmacological Basis of Therapeutics*, New York: McGraw-Hill, 2005.

32. Vogt, R. G., L. M. Riddiford and G. D. Prestwich, "Kinetic Properties of a Sex Pheromone-Degrading Enzyme: The Sensillar Esterase of Antheraea Polyphemus", *Proceedings of the National Academy of Sciences*, Vol. 82, No. 24, pp. 8827–8831, 1985.

33. Creighton, T. E., *Proteins: Structures and Molecular Properties*, Macmillan, 1993.

34. Alzate, O., *Neuroproteomics*, CRC Press, 2010.

35. Garrett, R. H. and C. M. Grisham, *Biochemistry*, Saunder's College Publishing London, 1999.

36. Michaelis, L. and M. L. Menten, "The Kinetics of Invertase Action (Translated by R. S. Goody and K. A. Johnson)", *Biochem. z*, Vol. 49, No. 333-369, p. 352, 1913.

37. Nicholls, J. G., A. R. Martin, P. A. Fuchs, D. A. Brown, M. E. Diamond and D. A. Weisblat, *From Neuron to Brain*, Sinauer Associates, 2012.

38. Wikipedia, "Acetylcholine — Wikipedia, The Free Encyclopedia", http://en.wikipedia.org/wiki/Acetylcholine, 2002, [Accessed June 2014].

39. "The Brain from Top to Bottom - the Role of Neuromuscular Junction in Muscle Contraction", http://thebrain.mcgill.ca/flash/a/a_06/a_06_m/a_06_m_mou/a_06_m_mou.html, 2011, [Accessed March 2014].

40. Heren, A. C., H. B. Yilmaz, C.-B. Chae and T. Tugcu, "Effect of Degradation in Molecular Communication: Impairment or Enhancement?", *arXiv preprint arXiv:1410.7895*, 2014.

41. Brown, R., *A Brief Account of Microscopical Observations Made in the Months of June, July and August 1827, on the Particles Contained in the Pollen of Plants, and on the General Existence of Active Molecules in Organic and Inorganic Bodies*, 1828.

42. Saxton, M. J., "Modeling 2D and 3D Diffusion", *Methods in Membrane Lipids*, pp. 295–321, Springer, 2007.

43. Moore, M. J. and T. Nakano, "Synchronization of Inhibitory Molecular Spike Oscillators", *Bio-Inspired Models of Networks, Information, and Computing Systems*, pp. 183–195, Springer, 2012.

44. Kuran, M. S., H. B. Yilmaz, T. Tugcu and I. F. Akyildiz, "Modulation Techniques for Communication via Diffusion in Nanonetworks", *Communications (ICC), 2011 IEEE International Conference on*, pp. 1–5, IEEE, 2011.

45. Yilmaz, H. B., A. C. Heren, T. Tugcu and C. B. Chae, "3-D Channel Characteristics for Molecular Communications with an Absorbing Receiver", *Communications Letters, IEEE*, Vol. 18, No. 6, pp. 929–932, 2014.

46. Radenovic, A., "Brownian Motion and Single Particle Tracking", http://lben.epfl.ch/files/content/sites/lben/files/users/179705/Brownian%

20Motion%20Handout.pdf, 2011, [Accessed February 2014].

47. Holden, J. and K. Kelly, "Brownian Motion", http://cnx.org/content/m14354/1.3/, 2007, [Accessed March 2014].

48. Perrin, J., *Brownian Movement and Molecular Reality*, Courier Dover Publications, 2013.

49. Einstein, A., *Investigations on the Theory of the Brownian Movement (Translated by A. D. Cowper)*, Courier Dover Publications, 1956.

50. Von Smoluchowski, M., "Zur Kinetischen Theorie der Brownschen Molekularbewegung und der Suspensionen", *Annalen der physik (in German)*, Vol. 326, No. 14, pp. 756–780, 1906.

51. Haw, M. D., "Colloidal Suspensions, Brownian Motion, Molecular Reality: A Short History", *Journal of physics: condensed matter*, Vol. 14, No. 33, p. 7769, 2002.

52. Fick, A., "V. On Liquid Diffusion", *The London, Edinburgh, and Dublin Philosophical Magazine and Journal of Science*, Vol. 10, No. 63, pp. 30–39, 1855.

53. Berg, H. C., *Random Walks in Biology*, Princeton University Press, 1993.

54. Stokes, G. G., *On the Effect of the Internal Friction of Fluids on the Motion of Pendulums*, Vol. 9, Pitt Press, 1851.

55. Tyrrell, H. J. V. and K. Harris, *Diffusion in Liquids: A Theoretical and Experimental Study*, 1984.